NASA CONTRACTOR REPORT

NASA CR-1232

CERTAIN PHYSICAL PROPERTIES AND APPLICATIONS OF NITINOL

by H. U. Schuerch

Prepared by
ASTRO RESEARCH CORPORATION
Santa Barbara, Calif.

NATIONAL AERONAUTICS AND SPACE ADMINISTRATION • WASHINGTON, D. C. • NOVEMBER 1968

CERTAIN PHYSICAL PROPERTIES AND APPLICATIONS OF NITINOL

By H. U. Schuerch

Issued by Originator as Report No. ARC-R-280

Prepared under Contract NAS 7-426 Mod 2
ASTRO RESEARCH CORPORATION
Santa Barbara, Calif.

for

NATIONAL AERONAUTICS AND SPACE ADMINISTRATION

For sale by the Clearinghouse for Federal Scientific and Technical Information
Springfield, Virginia 22151 – CFSTI price $3.00

SUMMARY

Experimental investigations have been performed of a number of physical properties of the nickel-titanium alloy known as Nitinol. The program was limited to wires and tapes of two specific compositions. Four types of tests were undertaken to characterize some of the thermomechanical memory effects observed in this alloy:

1) Stress-strain, for repeated load applications at constant temperature.

2) Temperature-elongation, for repeated temperature cycles at constant stress level.

3) Temperature-elongation for repeated temperature cycles at discontinuously variable stress levels simulating a thermodynamic power generation cycle.

4) Differential thermal analysis of unstressed samples for the complete transition temperature range during repeated cooling and heating cycles.

Based upon evaluation of the data obtained, a hypothesis of the deformation mechanism is postulated. Several engineering models demonstrating different applications of Nitinol were designed, fabricated, and tested. Descriptions of the physical properties characterized in the tests and of the various models and devices are presented in this report.

INTRODUCTION

Major technological progress is frequently triggered by the discovery of materials with unexpected and unusual physical properties. The development of solid-state electronics, based upon the properties of semiconductors, is an example. Of similar nature is the discovery of the unusual thermomechanical properties of certain intermetallic compounds, particularly those of the near stoichiometric composition of nickel and titanium (NiTi) as reported by Buehler, Wiley, Wang, and others (Refs. 1 - 14). The major portion of scientific work devoted to this material has been conducted by staff members of the Naval Ordnance Laboratory, Silver Spring, Maryland, hence the NiTi compound has been referred to as 55-Nitinol and 60-Nitinol* (Ref. 2). Of the two compositions, the near stoichiometric 55-Nitinol exhibits unique thermomechanical properties associated with reversible dimensional changes.

The work reported here was undertaken in an attempt to characterize some of the particularly intriguing properties of this material and to review concepts of structural-mechanical applications which could employ those properties.

In an effort to establish the feasibility of several usages, engineering models were designed, fabricated, and tested. The applications considered were all associated with solar heating in a space environment. The conversion of thermal energy into mechanical work by the Nitinol was adapted to the movement of shutters, to the bending of a spring, and to the rotation of a shaft. Tests of the engineering models were performed in a simulated space environment or in air at ambient conditions. Solar heating and space cooling were simulated by electric heaters, and by radiation or convective cooling.

---

* The numerical prefix refers to the weight percentage of nickel (atomic weight 58.7) the balance being titanium (atomic weight 47.9) and impurities, if any. Hence a pure stoichiometric (50 atomic percent) NiTi composition will have a nickel content very close to 55 percent by weight.

REVIEW OF CRYSTALLOGRAPHIC AND PHYSICAL PROPERTIES

A group of remarkable properties were found for the intermetallic compound NiTi in the course of an investigation of the NiTi alloy system at the Naval Ordnance Laboratory, White Oak, Maryland. Many of these properties are related to order-disorder transitions which occur in the near vicinity of room temperature, and include tensile elongations up to 20 percent, retention of extreme ductility at cryogenic temperatures, remarkable fatigue resistance and damping characteristics, and an apparent "memory" effect such that a part deformed at a temperature below the transition temperature will revert to its original form on heating to the transition temperature. As alloy compositions are varied from 55 to 60 weight percent of Ni, the alloys vary from soft and non-hardenable to those which can be hardened to an Rc hardness of 62. In addition, all compositions appear to be non-magnetic.

The order-disorder transition temperature of the intermetallic compound NiTi is dependent on the precise alloy composition. As the composition varies from 50 to 53 atomic percent Ni, the transition temperature in stress-free materials decreases from 165°C to -50°C, while at 47 atomic percent Ni the transition temperature decreases to 100°C.

The intermetallic compound has a body-centered cubic CsCl type of structure with an $a_o = 9$ Å superlattice and an $a_o = 3$ Å sublattice. This atomic arrangement has four possible orientations which are statistically distributed with extremely short-range order. Above the transition temperature the sublattice structure is ordered and the superlattice structure disordered. As the temperature is lowered through the transition temperature a martensitic-type, diffusionless transition occurs. In this transition the atoms shift positions cooperatively by a distance up to 0.8 Å, accompanied by an exothermic heat effect of 5.78 cal/g. After this transition the $a_o = 9$ Å superlattice is ordered, and the $a_o = 3$ Å sublattice is disordered.

Associated with this transition the NiTi intermetallic compound possesses a "memory". Materials plastically deformed below the transition temperature recover their original shape on heating beyond the transition temperature. Since this is a diffusionless transition, this change can occur very rapidly,

depending on heating rates, etc. Surprisingly large forces are developed by material deformed below the transition temperature and constrained during heating. Tensile stresses as high as 67 000 psi have been observed in wires that are heated past the transition temperature while constrained by rigid clamps. Wang has shown in recent work that the transition temperature is related to free electron concentration. This is also consistent with observed large changes in electrical resistivity (up to 50 percent) at the transition temperature.

Because of the limited amount of engineering data available for this material, a preliminary experimental program was undertaken to characterize some of the thermomechanical properties of 55-Nitinol wire. These results indicate that the mechanical manifestation (i.e., the discontinuous dimensional change associated with the transition) is a strong function of applied stress. In fact, two distinct temperatures at which dimensional changes occur are observed in samples subject to tensile stress. A higher transition temperature is obtained during the heating cycle; a lower transition temperature is obtained during cooling.

Investigation of the stress-strain properties of annealed 55-Nitinol wire at constant temperature below transition shows a very low apparent yield threshold followed by large elongation (6 percent) at approximately constant stress. This is followed by a marked increase in modulus with relatively small plastic deformations to high stress levels prior to fracture. This strain-hardening effect appears to be unidirectional inasmuch as upon stress reversal in bending and torsion experiments, large reverse deformations at low stress levels are again obtained.

Finally, it has been shown that stressed material is capable not only of recovering mechanical energy expended during the quasiductile deformation below the transition temperature, but that a portion of the latent heat of transformation becomes available in the form of mechanical energy. Hence, the material can be considered as "solid state working fluid" in the sense of thermodynamic power generators.

Several typical properties of the near stoichiometric NiTi intermetallic compound 55-Nitinol (55 weight percent Ni) taken from Reference 2 are listed below.

(a) General Physical Properties

Density - 6.45 g/cm^3

Melting point - 1310°C

Magnetic permeability - <1.002

Electrical resistivity - ~80 μ ohm cm at 20°C

- ~132 μ ohm cm at 900°C

Mean coefficient of thermal expansion - 10.4 x 10^{-6}/°C (24° - 900°C)

Forming - conventional hot working directly from arc-melted ingot at temperatures of 700°C to 950°C. Room temperature working possible with intermediate anneals at 800°C.

(b) Mechanical Properties at Room Temperature (below transition temperature)

Ultimate tensile strength - 125 000 psi

Yield strength, 0.2% offset - 30 000 psi

Total elongation - 22%

Reduction in area - 20%

Impact, unnotched - 117 ft-lb (20°C)

- 70 ft-lb (-80°C)

- 155 ft-lb*(20°C)

- 160 ft-lb*(-80°C)

Fatigue - (R.R. Moore - no failure in 25 x 10^6 cycles, 70 000 psi rotating beam test)

---

* 55.1 weight percent Ni; 44.8 Ti; 0.08 Fe.

The thermomechanical properties, particularly of the 55-Nitinol compounds, cannot be explained solely on the basis of either the nature of covalent bonding in intermetallics or by the conventional dislocation theory of ductility in metals. Neither are analogies derived from the rheology of thermoplastics and rubber materials fully satisfactory. Indeed, no theoretical basis appears to be available at this time which is consistent with all experimental observations. No attempt will be made here to establish such a basis; however, several qualitative observations should be noted which are indicative of the nature of deformation mechanisms that could conceivably be involved.

Crystallographic studies by Wang suggest a simultaneous and cooperative movement of atoms in specific crystal planes as the transition temperature range is traversed. If such movements become directionally biased by applied mechanical stress, then the mechanism of crystallographic twinning suggests itself, and an explanation for the large quasiplastic ductility of the materials can be construed. Since such motions will involve simultaneously a very large number of atoms, they will not be activated but rather inhibited by thermal action. The lower the temperature, the easier it will be to stress-activate such motions; hence the materials' apparent "ductility" will be retained at low temperatures. Specifically, the ordering of the 9 Å superlattice below the transition temperature will alleviate resistance to this movement. Also, it may be expected that below the transition temperature covalent (i.e., space-oriented) bonds across adjacent layers will tend to be replaced by nonoriented metallic bonds. Evidence for this is found in the observed rapid decrease in electrical resistivity as the temperature is lowered through the transition region.

The crystal structure of stoichiometric NiTi (II) phase, reported by Wang, indicates linear atomic sequences of Ti-Ti-Ni-Ti-Ti and Ni-Ni-Ti-Ni-Ni in adjacent layers of the crystal structure. A somewhat simplified, two-dimensional model of this arrangement is shown in Figure 1, the smaller dark circles indicating the smaller (but heavier) nickel atoms, the larger white circles indicating the larger (but lighter) titanium atoms.

Figure 1a shows a hypothetical arrangement for an unstrained, fully annealed NiTi crystal at low temperature. Figure 1b shows the same crystal deformed by shear stress. The deformation involves cooperative movements of all atoms in a single row by a

fraction of atomic distance.

We note that further shearing motion in the direction of applied stress is inhibited by the impending interference or "conjunction" of two large titanium atoms in each unit cell of adjacent rows, thus limiting the extent of deformation at low stress levels. Reversal of stress at this level will again cause cooperative shearing motion at relatively low stress levels until titanium atom interference is again reached at the opposite end of the low-stress deformation domain. In brief, the postulated model provides two unidirectional "stops" to shearing motion, within which the material can deform at low levels of activating stress.

Further increases in stress will cause the material to behave essentially elastically until additional anelastic shearing motions become possible by breakthrough of the "stops" formed by the titanium conjunctions. Only such additional motions will then constitute permanent, irreversible deformations of the material in the normal metallurgical sense and provide a new macroscopic equilibrium shape to which the material will revert.

Let us now examine the effect of an increase in temperature. The relatively lighter titanium atoms will tend to vibrate at larger amplitudes around their equilibrium positions and thus exert a repulsive diagonal force along the conjunction stop. The statistically preferred arrangement now is one of randomly distributed left-right shifts of adjacent layers, as shown schematically in Figure 1c. We note that the systematic (macroscopic) shear deformation of Figure 1b has been removed. Further, we note that the thermal motion of the atoms (and the attendant disordering of the 9 Å superlattice) will tend to inhibit further quasiplastic deformations from this thermal equilibrium structure. It appears reasonable to expect that the temperature at which recovery occurs must increase with increasing stress.

The postulated cooperative limited-slip mechanism is suggestive of the twinning deformations of certain mineral crystals, but differs from the dislocation mobility mechanism in conventional metals. Hence, the initiation of cyclic fatigue cracks by dislocation pile-up at surfaces and barrier sites should not occur. The large macroscopic deformation at low stress levels also will provide an effective relief mechanism for stress concentrations at notches or incipient cracks. This is consistent with the apparent insensitivity of the material to low-cycle

fatigue in the plastic deformation range and consistent with its excellent notch-impact resistance.

Referring to Figure 1b, a slip motion of 0.8 Å will produce a maximum recoverable shearing angle of approximately 0.25 radian. From this, maximum recoverable deformation of the order of 12 percent axial elongation could be expected in single, perfectly oriented crystals. Actual measurements have shown recovery of up to 10 percent elongation which compares well with the predicted value.

The stress-induced ordering mechanism provided by the postulated titanium conjunction stop would explain the observed increase in temperature at which deformation recovery takes place in stressed samples. As the applied stress increases, higher thermal activation will be required to produce random arrangement of the adjacent layers.

If the deformation recovery is indeed a direct result of thermal short-range disordering of the 9 Å superlattice, it will be expected that unavoidable small cyclic variations in temperature in the vicinity of the transition temperature will cause the material's properties to undergo changes with aging and be particularly sensitive to the complete thermal history subsequent to the initial high-temperature annealing process.

Finally, some intriguing analogies with the thermoelastic behavior of rubber may be noted. In both cases, the thermal motion and tendency to randomized molecular arrangements appear to be responsible for the recovery of deformations. Also in both cases the degree of recoverable deformation is limited by mechanical interatomic bond constraints. This mechanical constraint is provided, in the case of NiTi, by the postulated titanium conjunction; in the case of rubber, by orientation (stress crystallization and removal of the rotational degrees of freedom) in randomly coiled polymer molecules.

The tentative deformation model concept described here is incomplete and crude at best. It does not, for instance, account satisfactorily for the electronic material's properties changes nor does it consider the effects of changes in the nature of chemical bonds which are obviously taking place during the transition. Regardless, it is compatible with some of the experimental observations.

A functional understanding of these mechanisms will have to be developed by further scientific studies to allow a full

development of the technological potential inherent in materials of the 55-Nitinol type.

TEST PROGRAM

Two types of 55-Nitinol were used in the test program:

Type	Wire Diameter (in.)	Composition*		
		C	Ni	Ti
I	0.026	0.07	Bal.	44.6
II	0.020	0.06	54.6	Bal.

Upon receipt at Astro Research Corporation, the Type I test material was conditioned by heating in vacuum to 522°C in 29 seconds, followed by 7.3 seconds at 522°C, then subsequent cooling.

For some of the tests the wire of both Types I and II was rolled to form strips measuring about 4 x 55 mils in an experimental rolling mill developed at Astro. The wire was heated before passing through the rollers. Reduction of area is achieved by multiple passes, with a final cold pass. Details of the strip fabrication process are given in Appendix A.

Stress-Strain Tests

Axial strain tests were conducted on both wire and strip samples, and torsional strain tests were conducted on wire. In the axial strain testing, a length of wire or strip was suspended from a clamp and loaded by attaching calibrated weights. Elongations were measured by a micrometer-mounted traveling microscope used to record the distance between two bench marks on the test sample. Loads were applied in equal increments at intervals of approximately 3 minutes with elongation readings made after

---

* From certified ladle analysis supplied by Special Metals Corp., Utica, New York

apparent motion had ceased. Details of the apparatus and procedures are given in Appendix B.

To perform the torsional strain tests, a wire specimen was clamped vertically between two chucks. Torsional moments were applied through a torque drum to the upper chuck. As each moment increment was applied, an electric vibrator was actuated to reduce friction effects at low load levels. Angular displacement was measured on the torque drum. Details of this test apparatus and the testing procedures are given in Appendix B.

Data derived from the axial stress-strain tests are shown in Figures 2 through 4. Figure 2 shows the axial stress-strain data for Type I Nitinol wire for six stress cycles at room temperature, followed by thermomechanical strain recovery and by an additional load cycle. In Figure 3 are shown similar curves for the same wire after the material had been stored under normal laboratory conditions for approximately 12 months. A remarkable increase in the initial yield point of the material was observed in the second set of tests, indicative of an aging effect in the material. This aging effect appears to be due to small temperature excursions in the vicinity of room temperature, to which the material is exposed during storage (Ref. 5).

Figure 4 shows stress-strain data for Type II ribbon. The ribbon was heated to 100°C between each cycle but no significant thermomechanical recovery was observed. The transition temperature was later determined to be approximately 150°C. The second and subsequent cycles showed essentially normal elastic behavior of the material.

Figures 5 and 6 show the torsional stress-versus-strain curves of Type I material, strain recovered at 100°C. For the purpose of these graphs, an effective average shear stress was defined as

$$\bar{\tau} = \frac{12M_T}{d^3\pi}$$

where M_T = applied torque (in-lb)

d = wire diameter (in.)

This assumes a fully plastic stress distribution of uniform circumferential shearing stress throughout the wire cross section. The shearing angle, γ_{max} , is defined at the surface of the wire from

$$\gamma_{max} = \theta \frac{d}{2\ell}$$

where θ = relative angle of rotation at bench-marked sections (radians)

ℓ = length of test specimen between bench marks (in.)

Data shown in Figure 5 were obtained by applying positive (clockwise) torque to the sample, removing the load, heating the sample to 100°C to effect strain recovery, and then reversing the torque direction.

Data shown in Figure 6 were obtained by applying load reversal in each cycle before strain recovery. In either case, recovery was obtained without measurable residual strain in the unloaded condition.

Temperature-Elongation Tests

A Nitinol wire sample of Type I was tested for axial strain as a function of temperature with several values of constant preload. The wire was heated and cooled in a liquid bath, and the strain measured for a constant preload weight. Details of the test apparatus and procedures are given in Appendix B.

To obtain axial strain, an optical image splitter was employed to measure changes in wire length. The following formula was used:

$$\epsilon = 100 \frac{\Delta\ell}{\ell}$$

where ϵ = axial strain in percent

ℓ = original wire length under preload at ambient temperature

$\Delta\ell$ = change of wire length at test temperature

The procedure was to adjust the temperature of the bath and take image-splitter readings at the new temperature. The temperature increments were varied, depending upon the proximity of the wire temperature to the transition region. After establishing the upper and lower transition temperatures at which large changes of wire length occurred, the temperature increments in these narrow bands were reduced in order to obtain close spacing of strain data points.

In a typical test, the sample was preloaded and the scale set for zero axial strain at ambient temperature (about 20°C). The sample was then cooled down to -50°C, recording axial strain at 5- to 10-degree increments in temperature. The sample was then heated up in increments to +150°C,again recording axial strain. In the case of the 40-pound preload, the upper temperature was increased to +165°C. After reaching the maximum temperature, the sample was again cooled down incrementally to ambient conditions.

Data points were obtained at preloads of 1, 5, 10, 20, 30, and 40 pounds. A summary plot of approximated strain-temperature "hysteresis loops" is given in Figure 7. In Figure 8 are plotted the upper and lower approximate transition temperatures as a function of preload for this wire sample.

Thermomechanical Energy Conversion

These experiments were performed to measure the work done by Type I Nitinol wire during load-temperature cycling. A Nitinol wire sample having a diameter of 0.026 in. and a length of 13.30 in. was used. The wire was first loaded with 30 pounds at ambient temperature. It was then heated to above the upper transition temperature, causing the sample to contract by strain recovery. Then the load was reduced to 10 pounds, causing some additional strain recovery at constant temperature. Then the wire was cooled to room temperature. As the wire temperature traversed the transition region of approximately 40°C, elongation at constant stress was observed. Finally, the preload was restored to the original 30 lb which brought the wire back to its original condition of load and elongation.

The work performed is the load multiplied by the contraction of the Nitinol wire. As shown in Figure 9, two runs were made

with good repeatability. The useful work computed for the two runs was 11.0 and 10.8 in-lb, respectively.

Differential Thermal Tests

Using a Perkin-Elmer Differential Scanning Calorimeter, a series of runs was made on two samples of Type I wire to observe heat effects. Each sample consisted of five lengths of wire, each approximately 0.25 in. long. Total sample weights were 51.60 and 56.13 mg, respectively. Samples were encapsulated in standard Perkin-Elmer aluminum sample pans and run in a nitrogen atmosphere at a temperature scan speed of 10°C per minute, with a full-scale thermal sensitivity of 0.008 calorie per second. The temperature and sign of changes in latent heat were observed, quantitative heat changes calculated where possible, and heat capacity calculated at several temperatures. The values determined for specific heat are tabulated below:

°C	Specific Heat cal/gram-deg.
-48	0.110
-23	0.109
+77	0.109
+97	0.111
+437	0.113

TABLE I. SPECIFIC HEAT - TYPE I NITINOL WIRE

These values for specific heat are close to the value expected by comparison with titanium and with nickel; the increase with increasing temperature also appears normal.

Measurement of heat effects during temperature cycling shows that both the characteristic temperature and the magnitude of the heat effects are affected by thermal history. When cycling temperature within the overall temperature range of -80° to +500°C, it is found that changes in latent heat occur between -40° and +54°C.

On heating, starting from -80°C, either one or two endothermic transitions occur, both occurring over a narrow temperature range, one centered at +47° and the second at +54°. Occurrence of the peak at +47° apparently depends on prior thermal history. On cooling, up to three exothermic transitions are observed between +47° and -40°, again depending on prior thermal history.

The details of several temperature cycles, run using the two separate test samples, are shown in Table II.

		Heat Effect	Peak Shape	Temp. °C	Δ H cal/g
	Sample 1				
1)	Anneal in vacuum at 522° Store 4 months				
2)	Cool, +25 to -80°	exo	broad	-40	1.26
3)	Heat, -80 to +140°	endo	sharp	+47	-
			v. sharp	+54	
	Sample 2				
1)	Anneal in vacuum at 522° Store 4 months				
2)	Heat, +20 to +161°	endo	sharp	ca +54	-
3)	Cool, +161 to +15°	exo	sharp	+45	-
4)	Heat, +15 to +80°	endo	sharp	+54	1.53
5)	Cool, +95 to -80°	exo	sharp	+44	2.08
		exo	broad	-40	2.14
6)	Heat, -80 to +160°	endo	sharp	+47	4.74
			v. sharp	+54	
7)	Heat to 300°				
8)	Cool, +100 to -80°	exo	sharp	+47	>2.08
		exo	broad	-40	ca 2.14
9)	Heat, -80 to +100°	endo	sharp	+47	>4.74
			v. sharp	+54	
10)	Heat, +100 to 500°	none			
11)	Cool, +100 to -60°	exo	sharp	+39	2.21
		exo	medium	- 2	3.29
		exo	medium	- 8	
12)	Heat, -60 to +100°	endo	sharp	+54	5.56

TABLE II. DIFFERENTIAL THERMAL DATA - TYPE I NITINOL WIRE

APPLICATIONS OF NITINOL TO DEPLOYABLE STRUCTURES AND TO MECHANISMS

Design Concepts

Design concepts for applications of the thermomechanical memory effects of Nitinol can be categorized by reference to two types of characteristics. The first two described below refer to the specific functioning of the Nitinol element; the second two refer to the systems requirements in which the Nitinol element is to operate.

Nature of Mechanical Effect. - The thermomechanical memory effect can be employed to produce a desired displacement, as shown schematically in Figure 10a. Such displacements will be large compared to purely elastic deformations induced by loads. Alternatively, the effect may be employed primarily to generate a force, as shown in Figure 10b. Such a force, in turn, can be utilized to stabilize an otherwise collapsible structure, for instance, by pretensioning of brace wires or by clamping of joints.

Type of Deformation Employed. - For simple Nitinol elements, the type of deformation can be classified as illustrated in Figure 11: axial extension or compression, twist (or shear), and bending.

Source of Thermal Energy. - The thermomechanical effect requires a source of energy to produce the desired transition. Such energy can originate from the environment (i.e., solar heating); it may be supplied as a byproduct of the operating system (such as waste heat of electronic components or thermodynamic machinery); or it may be provided by an auxiliary system designed for this express purpose.

Operational Sequence. - This distinguishes applications in which a motion or force is produced only once during the operational cycle from those where repeated cycles are required during the lifetime of the device without special reconditioning of the material. Repeated cycling requires, in general, an elastic forcing member to work in cooperation with the thermomechanical recovery element, as shown schematically in Figure 12. This forcing device will provide the cold deformation at low temperatures. Deformations are then recovered upon heating, and restored upon cooling, in subsequent cycles.

A typical example for a deployable structure in the form of a hinged tube is shown in Figure 13. A familiar form of this basic concept is found in toys, where tubes and beads are strung together to form animal shapes which can be partially or fully erected and collapsed either by tensioning or relaxing the strings. In the concept shown here, the central string is made from a Nitinol wire which allows folding when stretched. Erection takes place when the axial stretching of the wire is recovered. The wire is strung over pulley segments such that tension in the wire will generate a hinge moment tending to straighten the joint. Rigidity of the deployed tube is obtained as the hinge flanges contact and the central wire tension is balanced by compression of the tube segments. A functional model of this device was fabricated and was found to operate satisfactorily.

The permissible ratio of pulley segment radius, r, to element length, L, is limited by the elongation recovery of the central wire, ϵ_R, i.e.,

$$\left(\frac{r}{L}\right) \leq \frac{\epsilon_R}{\pi}$$

This device employs a displacement effect (recovery of axial elongations in the wire) for deployment and a force effect for stabilization in the fully deployed condition. The source of activating energy can be environmental (exposure to sunlight after ejection from a shaded, cool container). Programmed deployment can be accomplished by selective heating of the central wire, for instance, by electrical resistance heating. The hinged tube concept is primarily a single-motion device. Repeated folding and unfolding is relatively simple, however, since cooling the central wire will allow refolding of the assembly by relatively small forces.

Another example of a Nitinol application is a telescoping tube which can be locked in its fully extended position by construction of pre-expanded NiTi rings (see Fig. 14). The actual deployment of the tube employs conventional means (such as pressurization). The function of the Nitinol locks is to ensure structural integrity when deployed, by positively swaging the detent stops at the end of the deployment motion. It is therefore clearly a single-motion application, to be used only once in operational applications. The thermomechanical memory element here acts as a force member and the force is generated by direct hoop stresses (circumferential elongation). Let t and R be the thickness

and radius, respectively, of a NiTi ring. Then the swaging pressure, p_S, exerted by the ring will be related to the thermomechanical hoop stress, σ_R, by

$$p_S = \frac{\sigma_R t}{R}$$

Experiments have shown that thermomechanical recovery stresses of approximately 60 000 psi can be sustained, hence for reasonable t/R ratios very substantial swaging pressures can be generated.

The source of activating energy can be environmental, but since timing of contraction is frequently critical, some auxiliary heating may be required to effect the locking action at the proper instant. A possible application of this device involves tubing to convey coolant or heating fluids, for instance, for thermal power generators. In this case, the temperature of the fluid may, as a by-product, provide the temperature required to maintain the locking and sealing pressure at the joints.

An example of a deployable structure utilizing Nitinol is the lattice structure in the form of a multi-stage column, as shown in Figure 15. This type of structure is currently considered for a range of space applications where relatively lightly loaded compression-resistant columns of long spans are required (Ref. 15). The folding and erection kinematics of this device involve the relative rotation of the transverse triangular frames. This rotation produces a shearing deformation of the three lattice panels that form the sides of the column, and the shearing deformation, in turn, is resisted by the diagonal wire bracings between the battens.

Analysis shows that for appropriately dimensioned panels, one of the two wires in each field needs to elongate by approximately 6 percent during the collapse motion. This extension can be provided by springs acting as force members in one set of diagonals. Alternatively, it can be accommodated by the recoverable axial deformability of NiTi wire without recourse to spring elements. If this extension is recovered in the fully extended position, the column will be stabilized since the contraction of the Nitinol wires will cause tension in the opposite diagonals.

Nitinol application concepts for deployable tubes using bending strain recovery are shown in Figure 16. Figure 16a shows a

thin-walled Nitinol tube that can be flattened by lateral compression. Axial ridges of the cross section facilitate this effect and keep the local bending strains within tolerable levels. This concept is patterned after a design conceived for purely elastic deformation, first proposed by Sintes (Ref. 16), but extends its applicability to tubes of much larger wall thickness since allowable recoverable strains are increased by one order of magnitude.

Figure 16b shows a concept where a thin tubular membrane is expanded by a coil spring. Local bending and twisting allows the coil spring to be flattened and the assembly subsequently to be rolled up.

Figure 16c shows the functional applications of the bi-stable scroll tube that consists of a flat strip which can be rolled up longitudinally for stowage but tends to roll transversely if deployed. Several practical applications of this concept have been found, using elastic materials. The use of Nitinol extends the applicability by allowing more massive constructions capable of carrying heavier loads, and smaller packaging volumes for a given design.

An example of a compression-resistant strut can be provided by an array of at least three longerons or a flexible, tension-resistant sheath pretensioned by a coaxial Nitinol coil spring. (See Fig. 17.) Axial compression of the spring collapses the longerons or the sheath. The ratio of fully expanded to fully-collapsed length, L/L_o, equals the ratio of coil wire diameter, d, to coil pitch, P_e, in expanded condition. If a coil spring is to be completely compressed, the d/P_e ratio is in turn proportional to the permissible elastic (or recoverable) shearing strain, γ, i.e.,

$$L/L_o = d/P_e = 2\pi^2 \gamma \left(\frac{D}{P_e}\right)^2$$

where D is the median coil diameter.

The large recoverable shearing strains in Nitinol allow attractive packaging ratios for relatively powerful coils. In addition, large constraint forces are not required since the coil is compressed at low temperatures.

Repeated cycling of the constrained coil concept is possible, for instance, by providing a coaxial weak tension spring made from conventional elastic material. Because of its open lattice construction the constrained-coil concept with discrete longeron wires is well suited to activation by solar heating. If the Nitinol coil is made from hollow tubing instead of solid rod, auxiliary heating by heat-transfer media can be easily accommodated.

Three functional models demonstrating different applications of Nitinol have been designed, fabricated, and tested. A system for actuation of temperature-control shutters using Nitinol wire has been patterned after a similar system on the Nimbus satellite which uses expansion of a liquid vapor. A sun seeker, in which a compression spring is bent in the direction of the sun by the contraction of the Nitinol wire has been demonstrated. A second sun follower in which a shaft is caused to rotate relative to the sun has also been fabricated and tested. Descriptions of these three models, their principles of operation, and the demonstration tests are presented.

Temperature Controlled Shutter

The purpose of this investigation was to explore the possibility of substituting a Nitinol wire and pulley shutter actuation system (Fig. 18) for the present Nimbus shutter actuation system, in order to increase reliability and to reduce weight and volume requirements. In order to determine if Nitinol material could be used for the design of an actual operating mechanism, a simulated model of the semi-passive temperature control of the Nimbus spacecraft, using Nitinol wire rather than a fluid as the actuating medium, was designed, fabricated, and tested. Available 55-Nitinol wire, which has lower and upper transition temperatures as shown in Figure 8 does not meet the temperature requirements of the Nimbus spacecraft. However, the principle of operation was demonstrated, and a Nitinol composition with a smaller transition temperature range would render this device applicable to the Nimbus spacecraft.

Semi-passive temperature control is utilized in the Nimbus spacecraft for control of temperature in a number of its instrumented compartments (Ref. 17). The controlling mechanism consists of movable shutters positioned between the panel surface to be controlled, and cold space. Shutter movement exposes more or less

of the radiating panel surface area to vary the heat rejection as a function of panel temperature. Opening and closing of the shutters is equivalent to an effective emissivity range of 0.15 to 0.65. The shutters are enclosed in a box-like structure to prevent sun impingement.

In the Nimbus device the panel surface temperature is sensed by a tube soldered to the panel and containing a liquid-vapor mixture of Freon 11. One end of the tube is sealed; the other end is connected to a bellows actuator having a spring-loaded return. Motion of the bellows actuates the shutters. As the temperature of the panel rises, the temperature of the liquid also rises and increases the vapor pressure within the tube and bellows, causing the bellows to move out against the load of the return spring and to rotate the shutters until a balanced position is reached. The temperature control is designed to fully close the shutters at 25°C and fully open them at 35°C panel surface temperature.

The philosophy of the Nitinol model design was to construct a device which would simulate the operating principles of the semi-passive Nimbus temperature-control system without necessarily being an exact replica of the system. The model shown in Figure 18 consists of a wooden box, open on one end, with the shutters installed in the open end. A 0.063 in. thick copper plate (Fig. 19) separates the box into two approximately equal compartments. The closed compartment was lined with aluminized Mylar and an electric heating element installed in it to simulate the heat from electronic components. Since the model will be operating in a vacuum, the only means of heat transfer from the plate to the wire is by radiation. To increase radiation heating, copper tubes 1/8 O.D. x 0.035 wall were soldered to the plate between the pulleys, and the Nitinol wire was run through the center of the tubes. With this design, heat is conducted from the plate through the walls of the tube and then radiated to the wire from the inner surface of the tube. The exterior surface of the tubes was coated with a 1/16 in. layer of silicone rubber insulation (RTV 751) to prevent excessive heat loss from the exterior surface of the tube.

Calculation of the heat-transfer rate and the time required for the shutters to go from 0° to 90° is plotted in Figure 20. Calculations are also shown for a flat wire of 0.005 x 0.1 in. cross section (the same cross-sectional area as the 0.026 in. diameter wire) and for a 0.001 x 0.1 in. cross-section wire. The time constant of the flat wire is approximately half that of the round wire with the same cross-sectional area. For flat wire, the time

constant is directly proportional to thickness. In the data plotted in Figure 20, it was assumed that due to the high heat conductivity of copper, the temperature of the copper tube was constant around its circumference and the same temperature as the plate.

Type I Nitinol wire, 0.026 in. diameter, with a preload of 10 pounds, was selected for these tests. Strain-temperature data for this wire is shown in Figure 7. Since the transition temperature increases with tension, it was necessary to have constant tension on the wire during these tests in order to use this data. Since, with ordinary coil springs an increase in length required an increase in tension, the shutter drive pulley was mounted eccentrically to obtain an approximately constant tension in the Nitinol wire. The amount of eccentricity required to give a constant tension of 10 pounds in the Nitinol wire at the shutter full-opened, full closed positions was determined. The maximum deviation from constant tension was computed to be 0.4 pound at the mid-point of shutter travel.

In the operation of the model, the heating element radiates to the copper plate, and the heat is conducted around the walls of the copper tube. The Nitinol wire inside the tube is heated by radiation from the tube. If the temperature of the Nitinol wire reaches its upper transition temperature, the Nitinol wire starts to contract. Contraction of the wire rotates the shutter pulley, starts to open the shutters, and extends the return spring. If the plate temperature continues to rise, the wire will contract approximately 5 percent of its effective length and open the shutters to 90°. If during the opening of the shutters a heat balance is reached between the heat radiated from the plate and the heat put in by the heating element, the shutter will stop opening. If the heat is again increased, the shutters will open farther; however, if the heat input is decreased, the shutters will not start to close until the Nitinol wire reaches its lower transition temperature and starts to extend.

The test model was placed in a bell jar (see Fig. 21) which could be evacuated to 60 microns by a vacuum and diffusion pump, to test the operation of the system under near-vacuum conditions. A cold wall, to absorb the heat radiated by the copper plate, was provided by a copper-tube coil placed around the model. Lexsol 408-M*, cooled by a second coil submerged in a Lexsol dry-ice bath,

---

* A low-freezing-temperature liquid.

was continuously circulated through the cooling coils by an electric motor-driven pump. A minimum cooling coil temperature of -20°C was provided by this means. Thermocouples attached to the front of the copper plate and to the inlet and outlet of the cooling coils, and connected through a selector switch to a Speedomax H recorder, were used to measure the temperature of those points.

The power input to the heating element was controlled by a Variac and measured by a wattmeter in the circuit. A pointer was installed on an extension of the shutter shaft and a dial attached to the top of the box to measure the shutter angle.

Test Procedure. - The model was placed in a bell jar and connected as shown in Figure 21. The bell jar was evacuated to a pressure of 60 microns, the circulating pump turned on, and dry ice added to the Lexsol bath until its temperature was reduced to -80°C. Readings were taken of the cooling-coil inlet and outlet temperatures and the tests started by turning the Variac dial to the desired voltage setting. The power input for each Variac setting was read on the wattmeter. Plate temperatures were read for every 5° of shutter opening or closing.

The model worked smoothly and operated the shutters from fully closed to fully open and back again. Three runs were made. The results are shown in graphical form in Figure 22. During run 1 the heat input was greater than the heat radiated from the plate even with the shutters completely open. With the lower heat input of run 2, a heat balance was achieved at the shutter opening of 30°, after which the temperature gradually dropped as the shutters opened until at 70° the heat input was increased and the temperature again increased. The high starting temperature of run 2 was caused by using a high heat input to bring the box up to temperature before the shutters started to move.

An input power of 20 watts was used throughout run 3. The temperature reached a constant value of 83°C after 127 minutes and remained at this temperature for 25 minutes while the shutter angle changed from 69° to a maximum of 71°.

The relatively high heat input used for run 1 gave data points approximately 20°C higher than the temperatures required for transition. From Figure 20, the time required should be 6 minutes, and the actual time was 5 minutes.

Comparison of the test data indicates that when the shutter

stabilized at a 70° angle in runs 2 and 3, the difference in temperature between the two tests is approximately 5°C. The temperature difference required to cycle the shutters from fully closed is approximately 55°C for both sets of data, so the system is marginal for temperature control of the Nimbus spacecraft. However, it appears that Nitinol-55 compositions can be developed which have smaller differences between the upper and lower transition temperatures than does the material used in this model.

Sun Seeker

The feasibility of using Nitinol wire to bend a spring column toward the sun was investigated. A model designed for operation in air at room temperature was fabricated and tested using photo flood lamps as a radiant heat source. A number of design improvements were considered, including the use of flat tapes instead of round wires, and the application of coatings to increase the equilibrium temperature of the Nitinol.

The Sun Seeker shown in Figures 23 and 24 consists of a compression spring which has three Nitinol wires evenly spaced about its outer periphery. The wires, under tension, are attached at frequent intervals along the spring and to end caps on the top and bottom of the spring. The end caps also provide a means of attaching the device to a spacecraft or to solar panels. The Nitinol wires on the side of the spring away from the sun must be shielded from the sun. When the longitudinal axis of the Sun Seeker is straight and pointed directly toward the sun, all of the Nitinol wires will be shielded and the axis will remain straight. If the axis of the device is slowly rotated to point away from the sun, the Nitinol wires on the side of the spring toward the sun will be exposed. As the angle of the sun relative to the wire increases, the temperature of the Nitinol wire increases until the transition temperature is reached, causing the wire to contract and bend the spring toward the sun. This reduces the angle of the sun to the Nitinol wire above the bend to below its critical angle (the angle below which transition will not occur). Thus the bend effectively starts at the bottom of the spring and moves progressively upward until the axis of the spacecraft to the sun reaches 90°. At this angle, the entire spring is bent in an arc of a circle.

If the rotation of the longitudinal axis of the device is stopped somewhere between 0° and 90° relative to the sun, the

bending of the spring will stop because the angle of portions of the Nitinol wire will be below the critical angle. If the rotation of the axis is now reversed, the temperature of the Nitinol wire will start to drop, and when the lower transition temperature is reached, the Nitinol wire will start to elongate and straighten out the curve. This will continue until the spring is straight and will then repeat the previous process in the opposite direction.

The model consists of five principal parts - compression spring, Nitinol wires, end caps, reflectors, and simulated solar panels. The model was designed to operate at room temperature, either in the atmosphere or in a vacuum, with a heat lamp as the source of radiant energy. It was necessary to select a preload for the Nitinol wire such that the lower transition temperature would be above average room temperature (20°C) and still not have so high an upper transition temperature that it would be difficult to operate with a heat lamp. A preload of 17 pounds per wire was selected to give a lower transition temperature of approximately 28°C and an upper transition temperature of approximately 95°C.

A tradeoff study was made of the number of Nitinol wires to be used. The resulting selection of three wires was based on the following factors:

1. The minimum number of wires which will keep the springs stable and operate in any angular position is three.

2. The minimum number of wires will give minimum spring loads and minimum spring strength.

3. With three wires all the wires are loaded at all times, while with more than three wires some of the wires will be slack when the spring is bent, requiring the taut wires to carry the entire spring load.

4. Increasing the number of wires increases the pointing accuracy. With only three wires the plane of the bend in the spring, at some angular positions, can be considerably out of plane with the sun. This can be partially alleviated by giving the wires a slight spiral.

The spring design for three 0.026 in. diameter Nitinol wires with a 17-lb preload on each wire is shown in Figure 24. The spring was designed with a wide space between the coils to allow

for the installation of the reflectors. The length of the spring was computed based upon a 90° deflection of the Sun Follower.

The reflecting surface of the reflectors was gold plated to increase the reflectivity of the relatively long-wavelength radiation from the heat lamp. The purpose of the reflectors is not only to increase the effective heating, but to shield the wires from radiation until they are in the correct position.

The Nitinol wires were fastened to the upper and lower end caps and to each coil of the spring while the spring was under the preload tension. The Nitinol wire was fastened to the spring by winding annealed stainless steel wire around the Nitinol wire and spring and then soft-soldering the stainless steel wire to the spring to hold it in place.

Sun Follower and Rotary Drive

A second Sun Follower configuration which also can operate as a continuous rotary drive was designed, fabricated, and tested. In this model, which is shown in Figure 25, heating of the Nitinol wires or tapes causes rotation of a shaft. The device will either rotate continuously from the effects of solar heating, or point in the azimuth plane of the sun.

Figure 26 shows a cutaway engineering layout of the Sun Follower. The principal components are the central shaft, the canted bearing plate, the Nitinol wires or tapes, the cylindrical shield, the lower end plate, and the upper end plate. The subassembly of the central shaft and lower end plate rotates relative to the assemblage of Nitinol wire, upper end plate, and canted bearing-plate outer housing and cylindrical shield.

In the mode of operation in which a continuous rotation results, the lower base plate is clamped with the canted bearing plate in a position so that neither fully stretched nor fully compressed springs are nearest to the sun. As the Nitinol ribbons or wire nearest the sun heat up to a temperature above the transition point, the contraction of the Nitinol stretches the spring and causes rotation of the assembly of the upper plate, Nitinol strips, and outer housing of the canted bearing plate. As the heated Nitinol wire rotates into the shadow of the cylindrical shield, it cools down and is stretched by the spring tension when the lower transition temperature is reached. The rotation is continuous;

its rate is dependent on the heating and cooling rate of the Nitinol strips.

In the mode of operation in which rotation follows the sun's motion in azimuth, the upper end plate is clamped with the Nitinol strips extending vertically upward or downward. The Nitinol strips nearest the sun will heat up and contract as the transition temperature is reached. The contraction forces the inner race of the canted bearing plate to rotate into a position of minimum spring length for the heated Nitinol strip. The central shaft and lower bearing plate are pinned to the inner race and rotate so that one point on the periphery of the lower base plate always points toward the sun.

A series of tests were conducted on this demonstration model using the setup shown in Figure 27. A 2-kilowatt electric radiant heater provided the heating source for the Nitinol strips. A fan in the base was used to blow cooling air through the louvres on to the strips shielded from the radiant heater. With 0.026 in. diameter Type I Nitinol wires, the pointing accuracy was within 10° for the mode of operation in which the upper end plate was clamped. The rotational speed with the lower base plate clamped was approximately 10 rpm. When the 3-mil ribbons of Nitinol were substituted for the wire, the pointing accuracy was improved, and the speed of rotation doubled. The unit was continuously rotated for 8 hours (approximately 5000 revolutions) without appreciable change in performance.

CONCLUSIONS

A wide range of applications for Nitinol materials appears to exist in a variety of structural and mechanical devices. For space systems applications, the potential of directly using environmental thermal energy to actuate required mechanical motions is attractive. Also attractive are the possibilities of designing "flexure-type" mechanisms which do not require bearings.

The material is basically metallic and should exhibit excellent resistance to hard vacuum, temperatures extremes, and radiation.

Further experimental work in characterizing and controlling the thermomechanical properties of Nitinol is required to permit the design and construction of reliable space hardware.

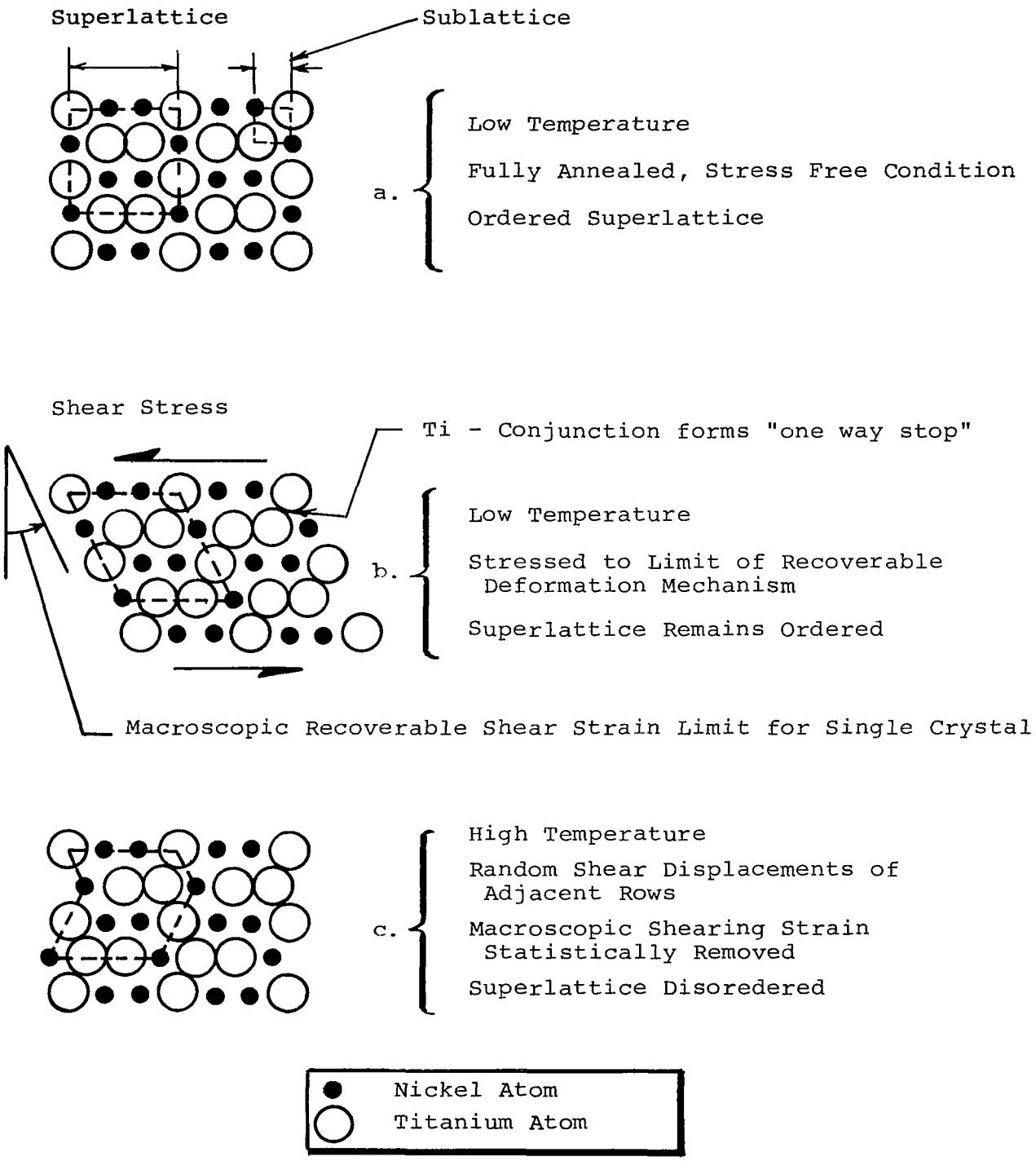

Figure 1. Conceptual Model of NiTi Deformation Hypothesis

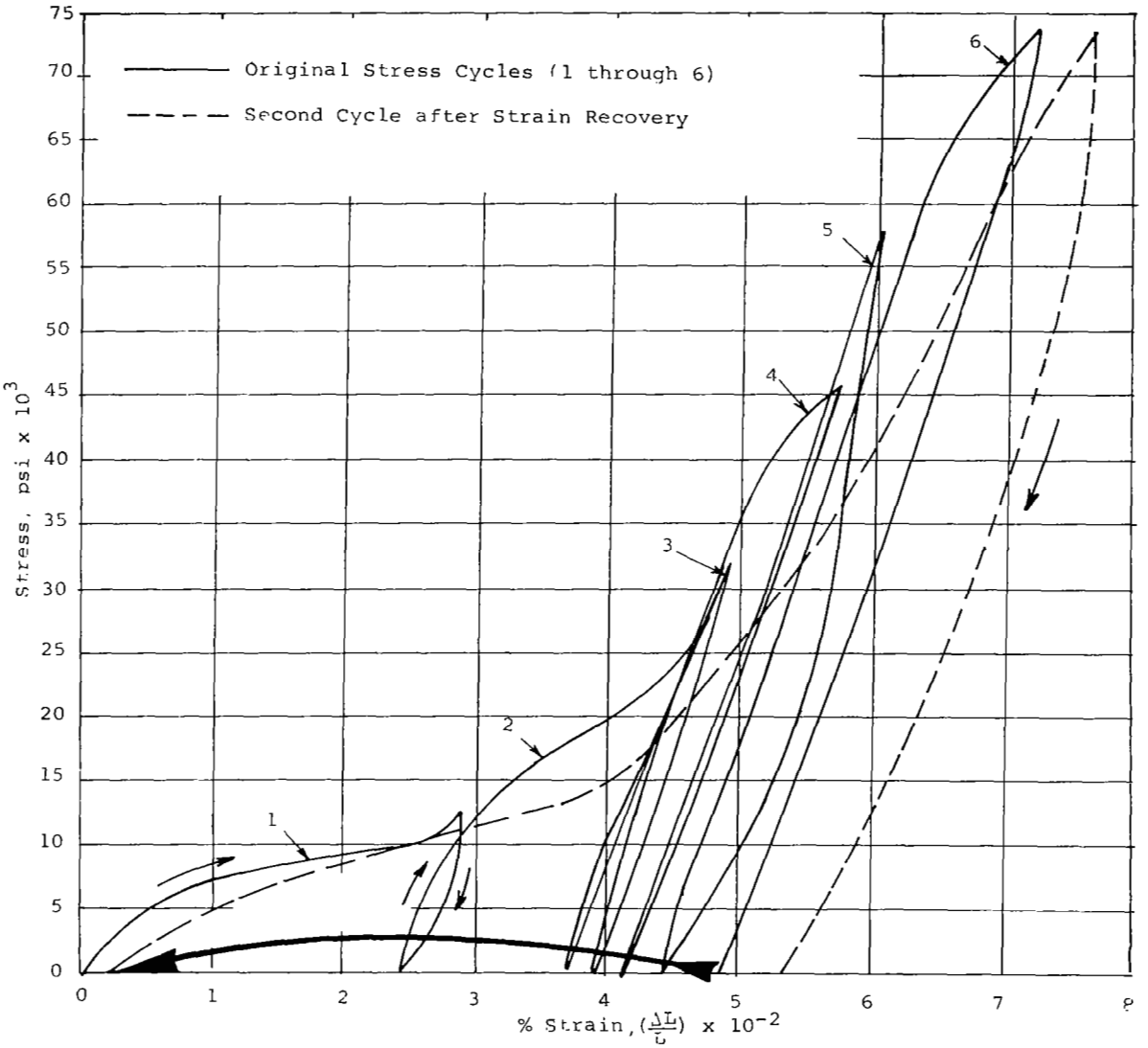

Figure 2. Axial Stress-Strain Data, Type I Nitinol Wire

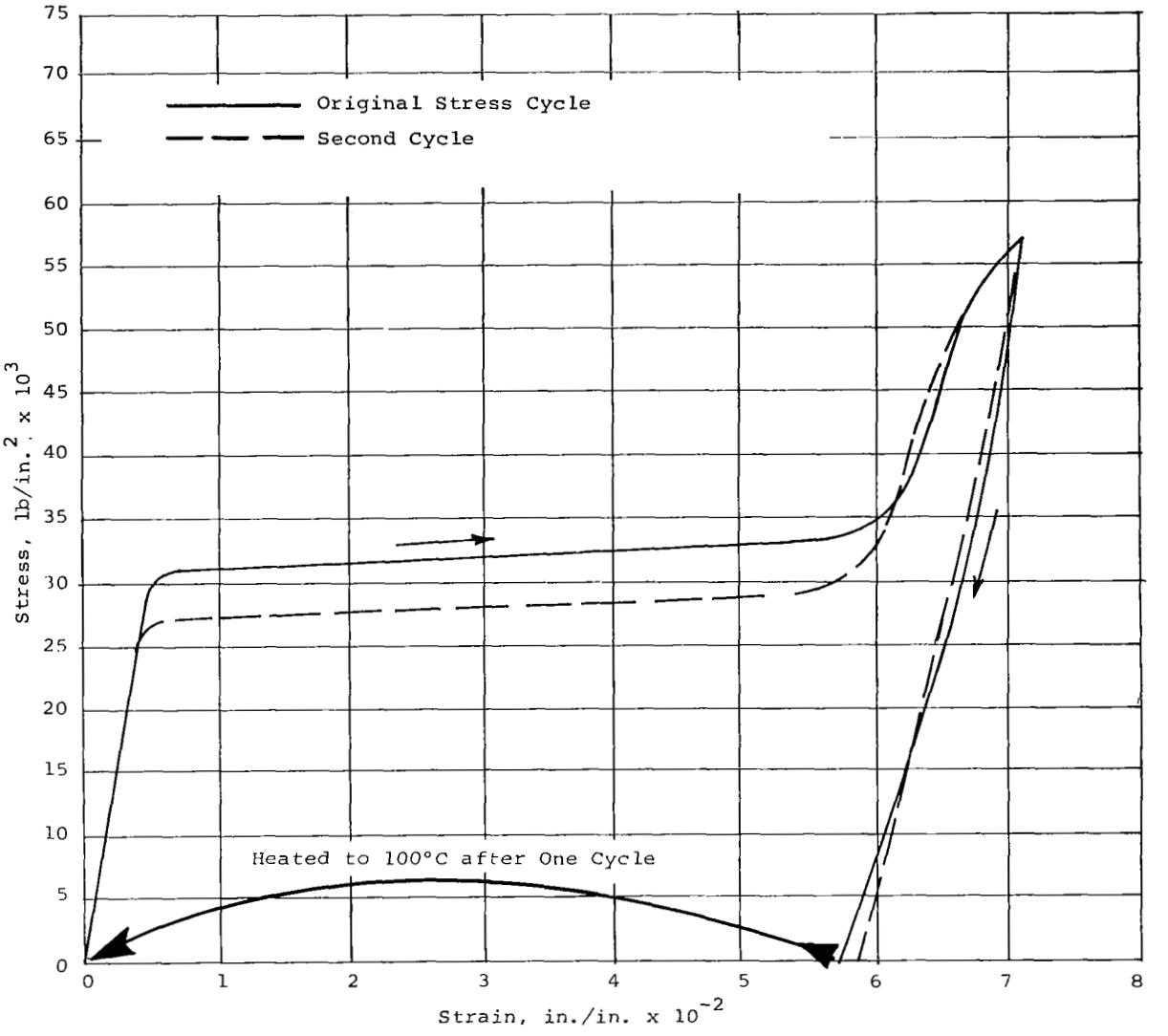

Figure 3. Axial Stress-Strain Data, Type I Nitinol Wire - Tested after 12 Months Storage

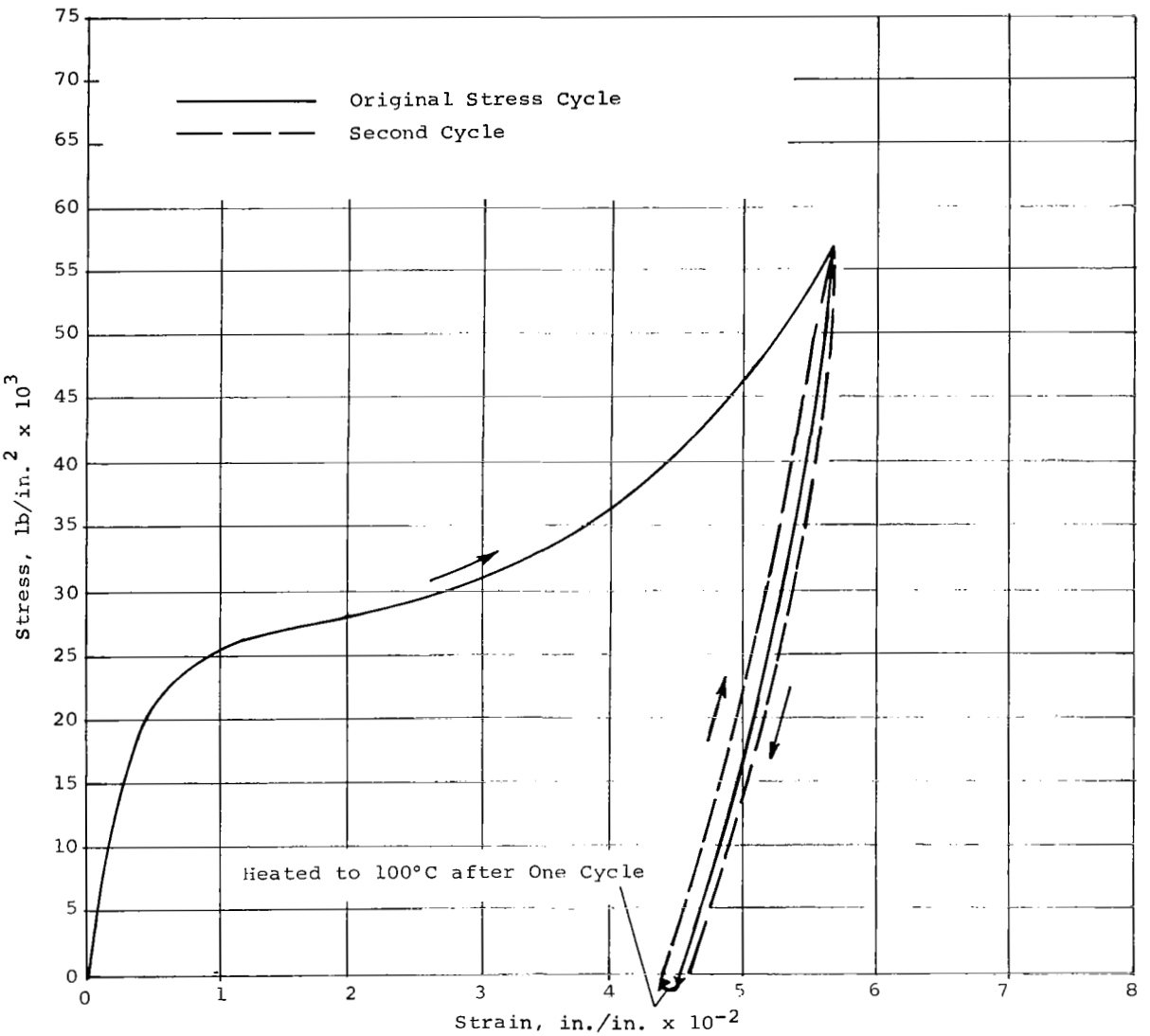

Figure 4. Axial Stress-Strain Data, Type II Nitinol Ribbon

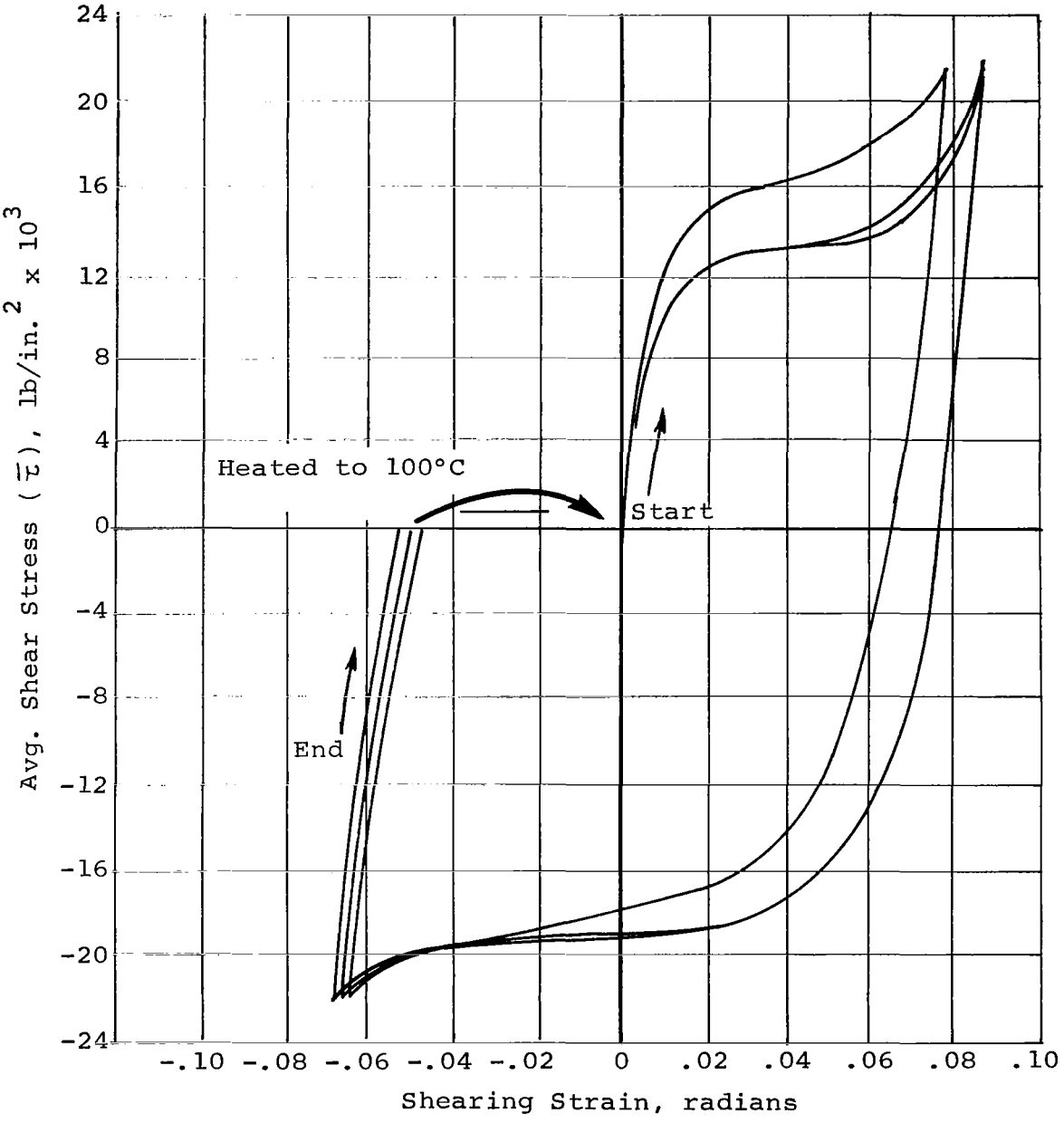

Figure 5. Torsional Stress-Strain Data, Type I Nitinol Wire, Strain Recovered after Each Stress Cycle

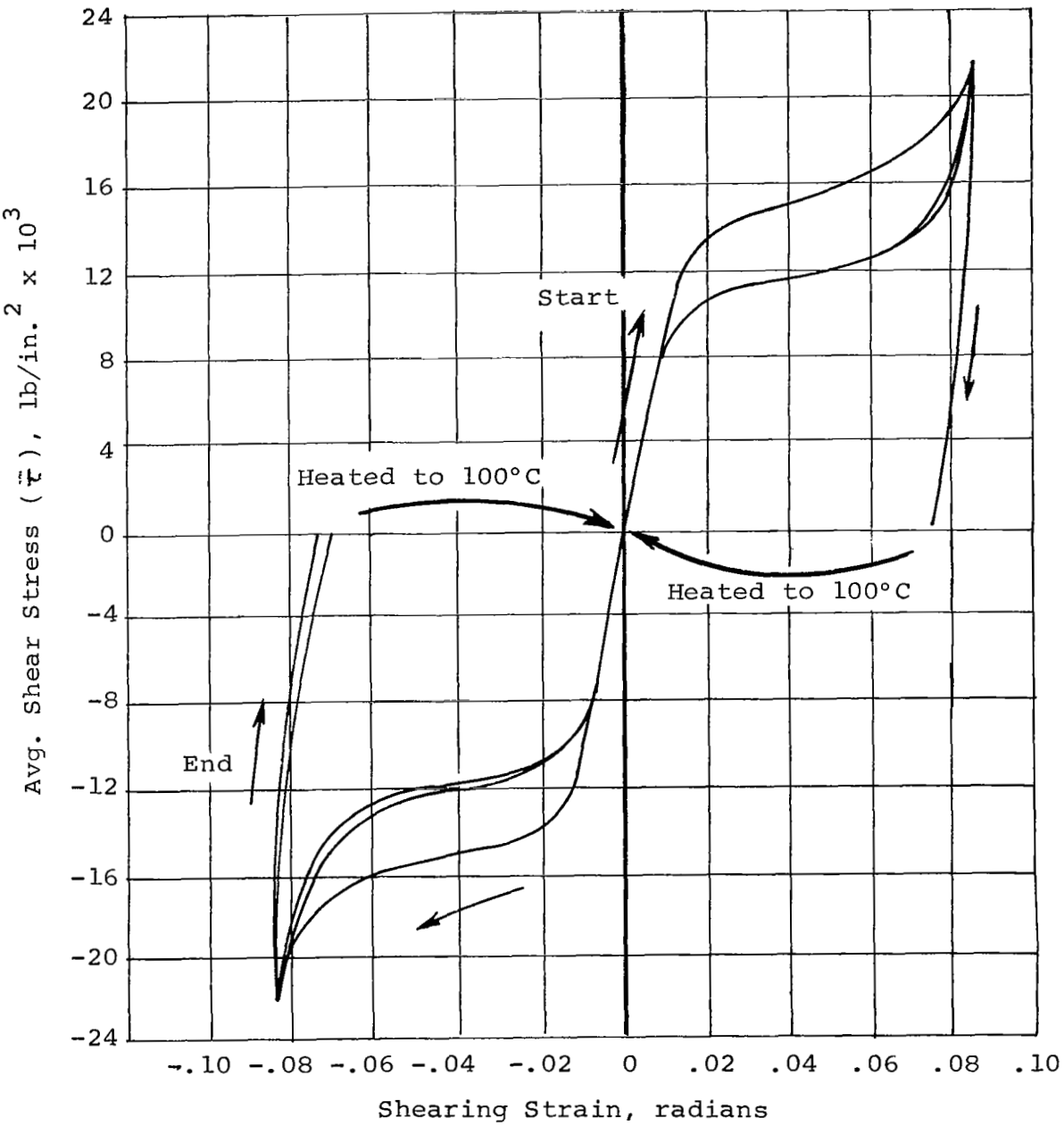

Figure 6. Torsional Stress-Strain Data, Type I Nitinol Wire Strain Recovered before Each Stress Reversal

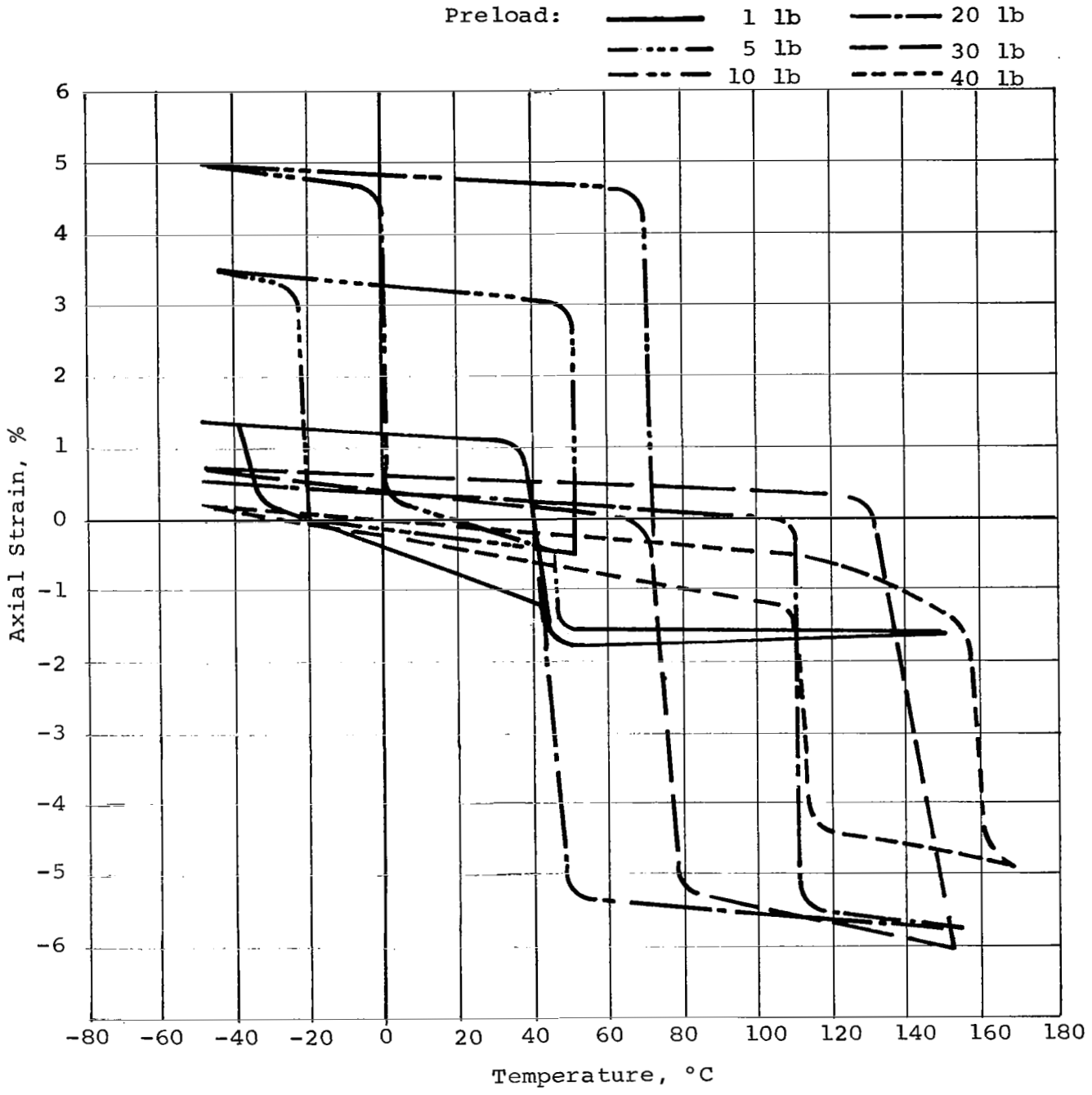

Figure 7. Summary of Strain Temperature Hysteresis
Type I Nitinol Wire

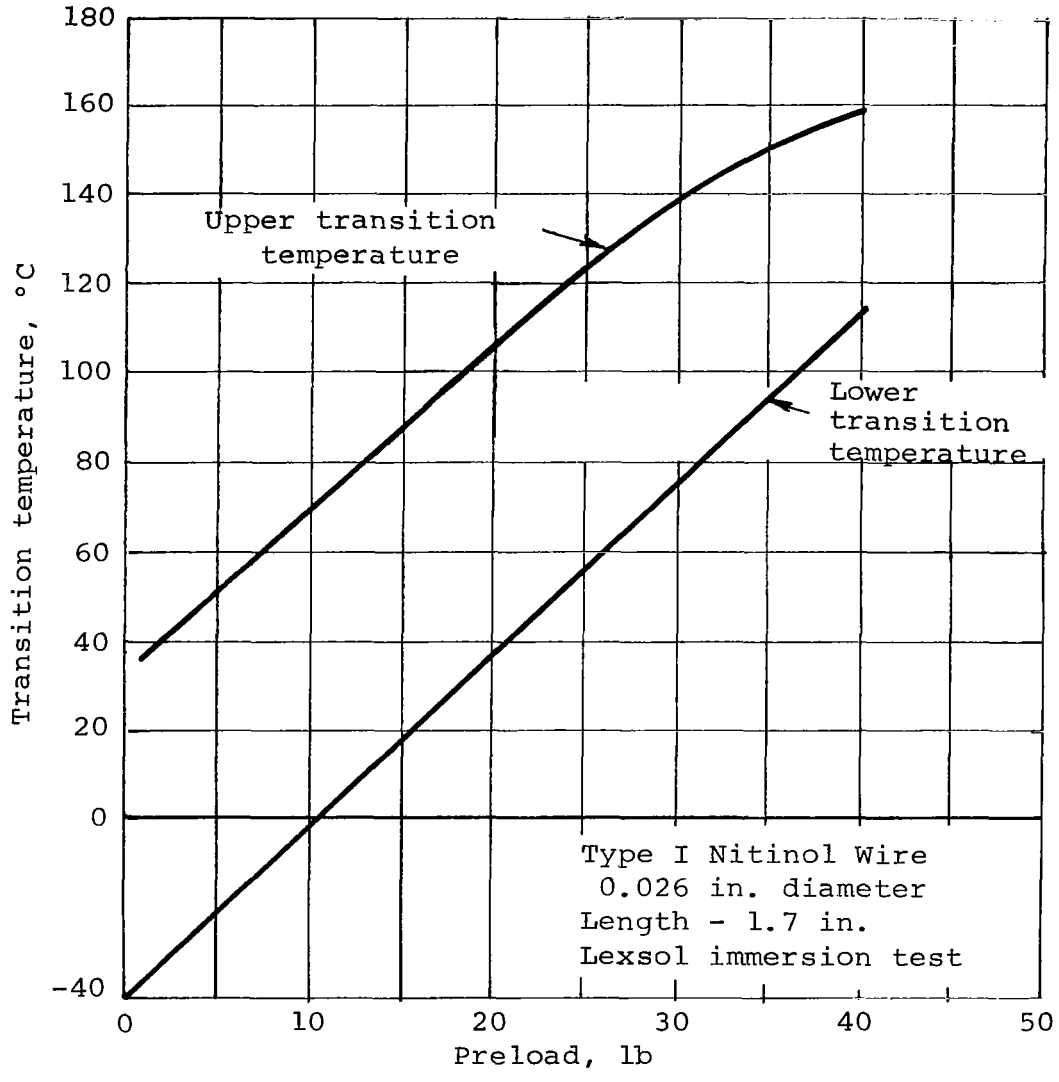

Figure 8. Transition Temperatures versus Preload Weight

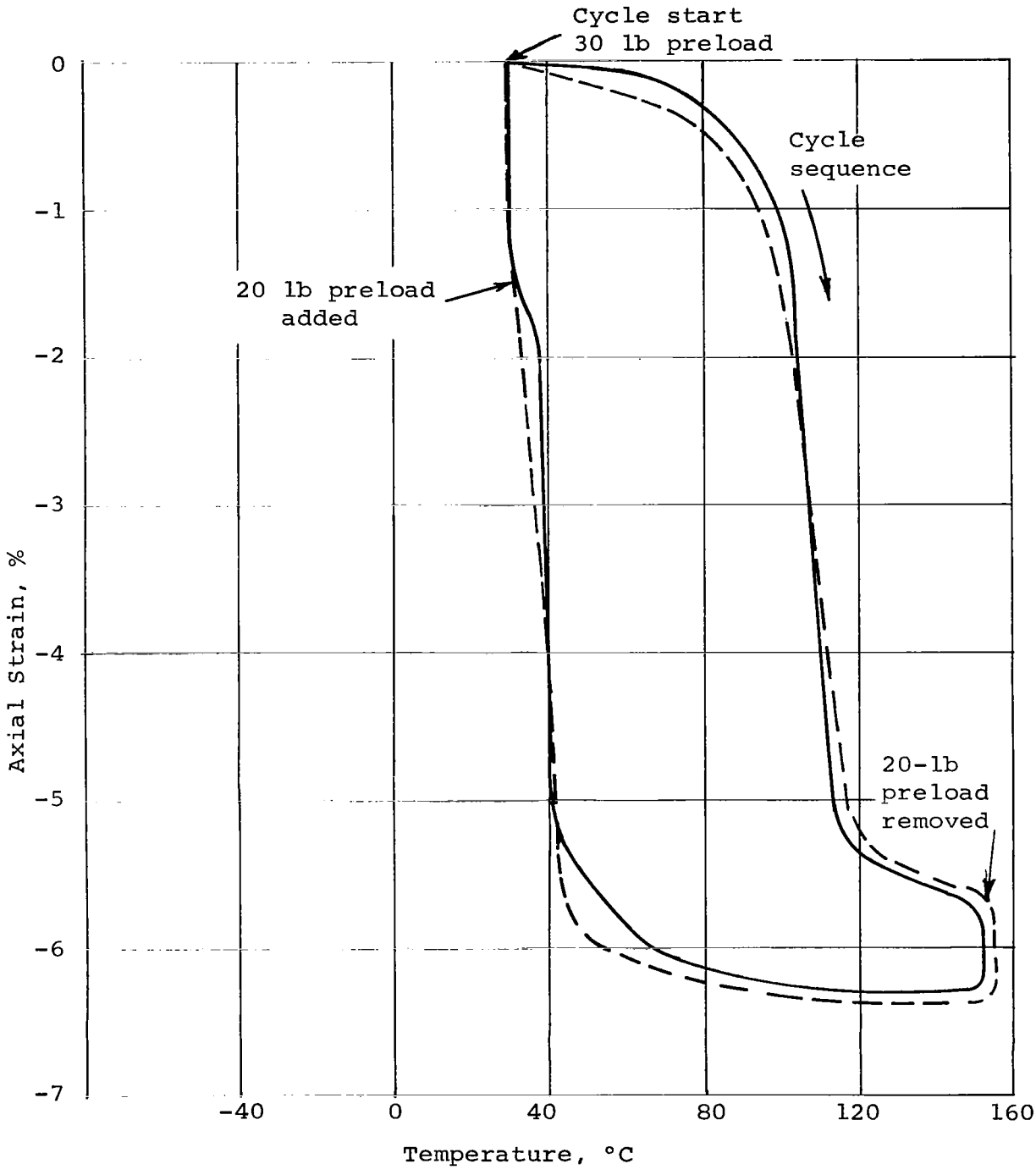

Figure 9. Temperature Elongation Data with Discontinuous Loading Type I Nitinol Wire

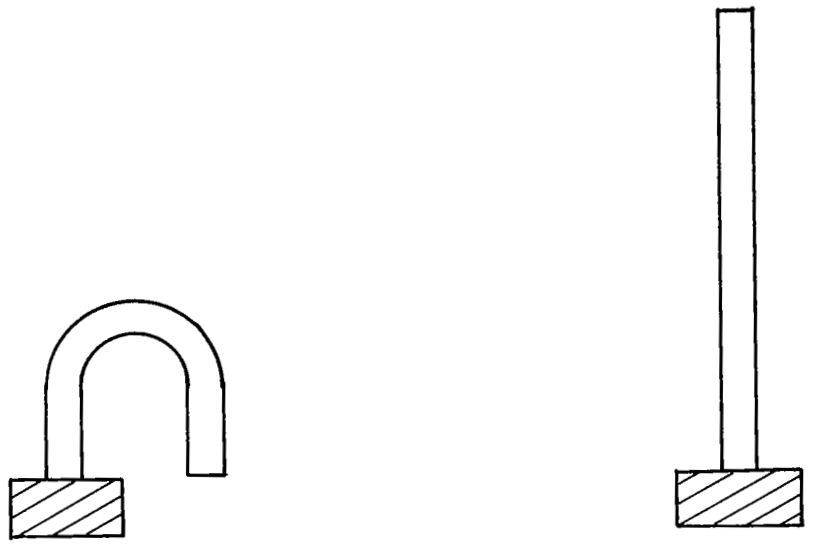

a. Displacement effect

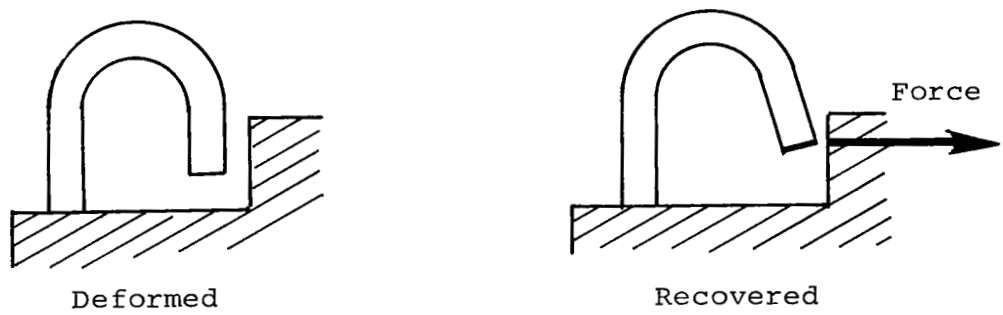

b. Force effect

Figure 10. Thermomechanical Recovery Effects of Nitinol

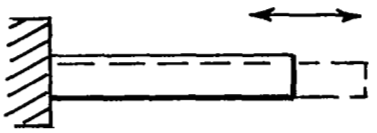

a. Axial extension

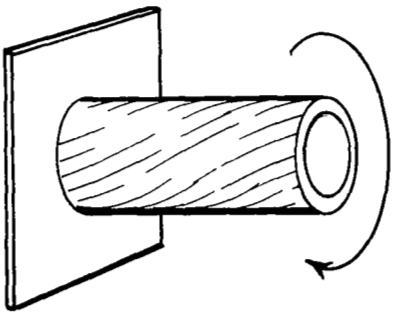

b. Twist

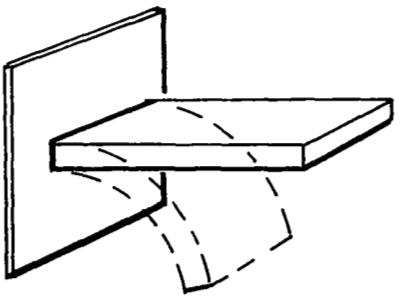

c. Bending

Figure 11. Types of Deformation

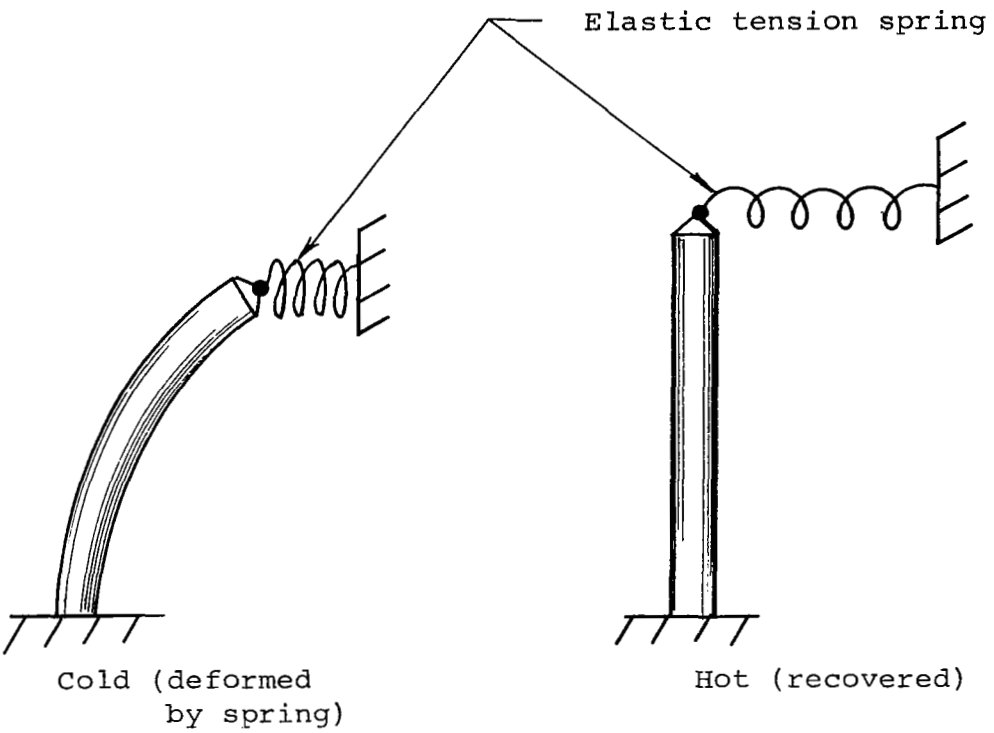

Figure 12. Schematic for Repeat Cycling of Nitinol Devices

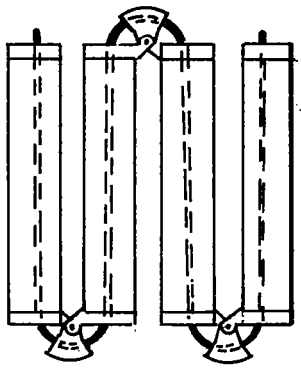

Folded

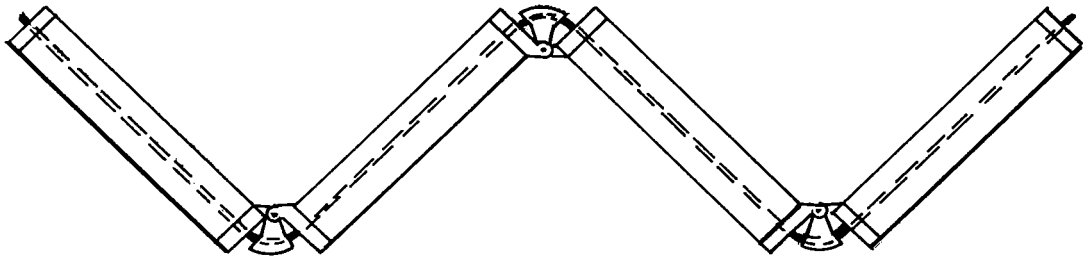

Contraction of Nitinol Wire

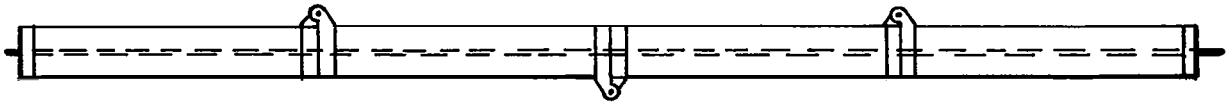

Deployed

Figure 13. Hinged Tube Application

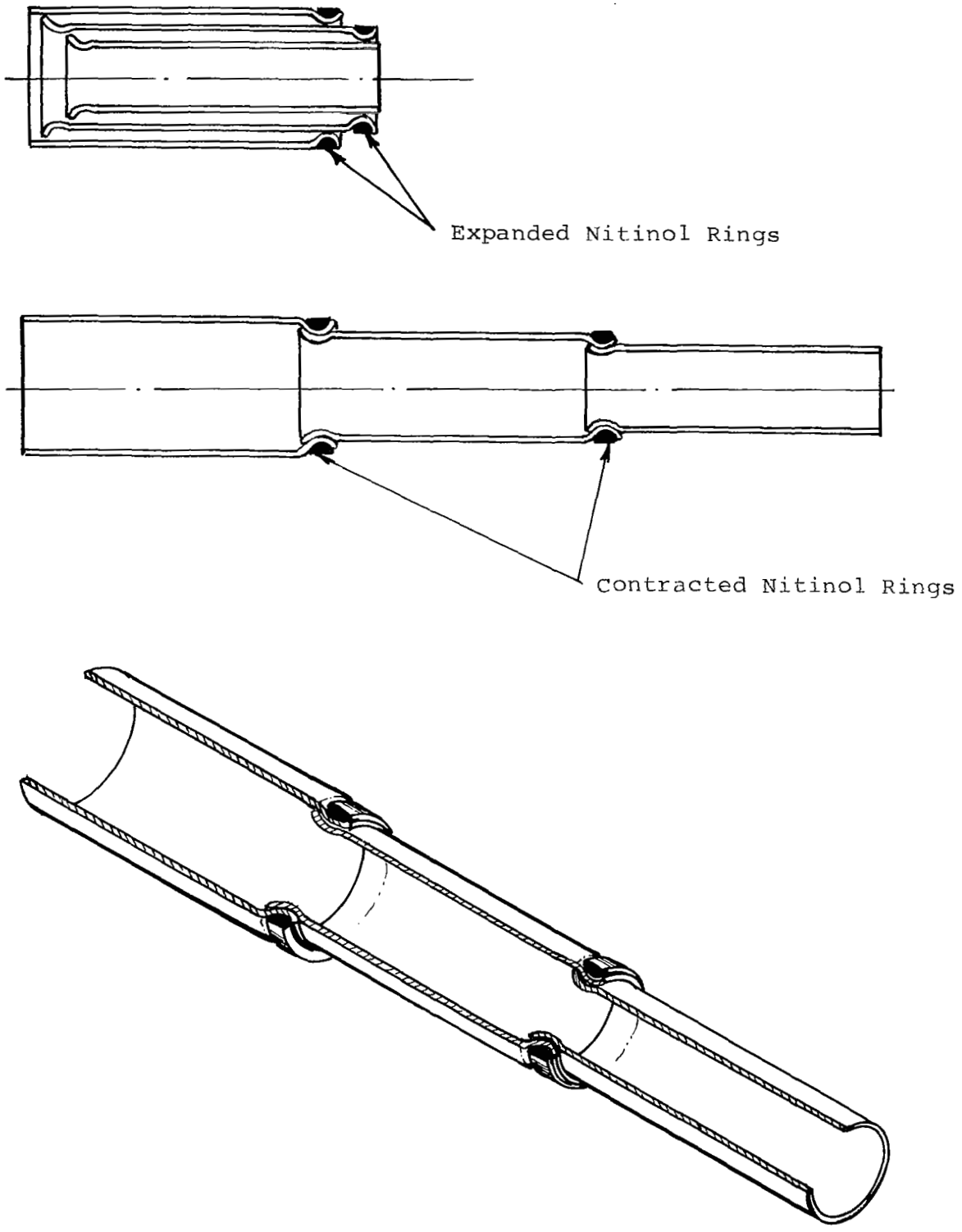

Figure 14. Telescoping Tube Joint Lock

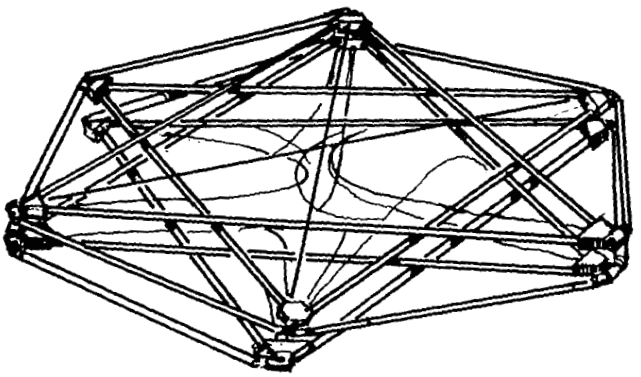

Folded

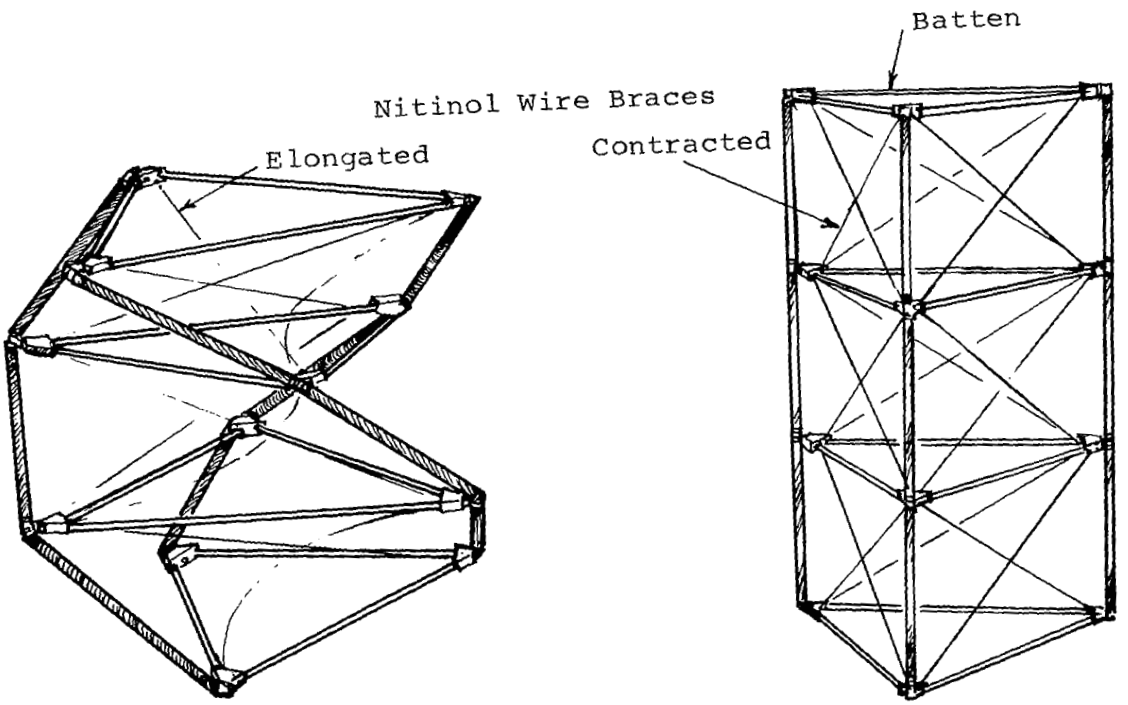

Figure 15. Nitinol Deployed Lattice Mast

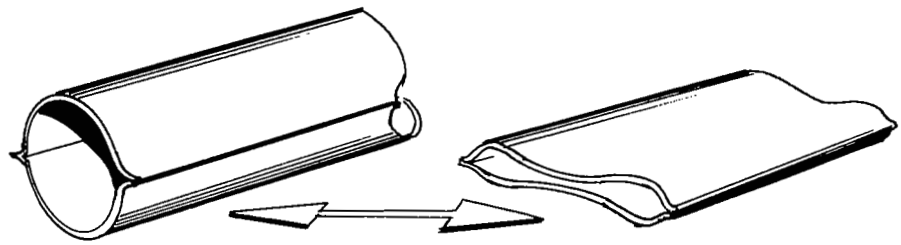

a.

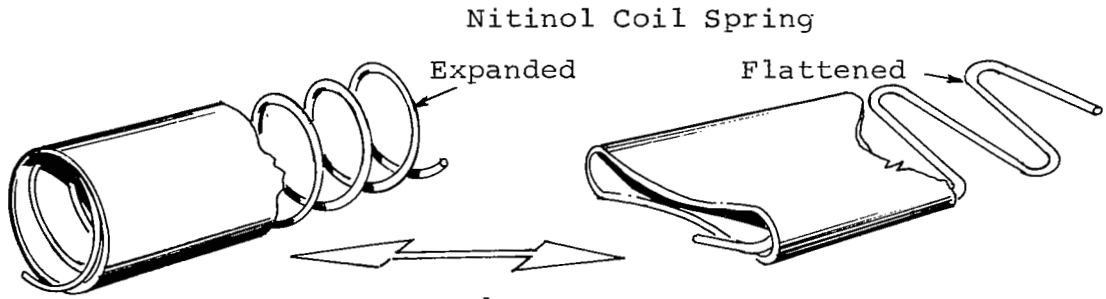

b.

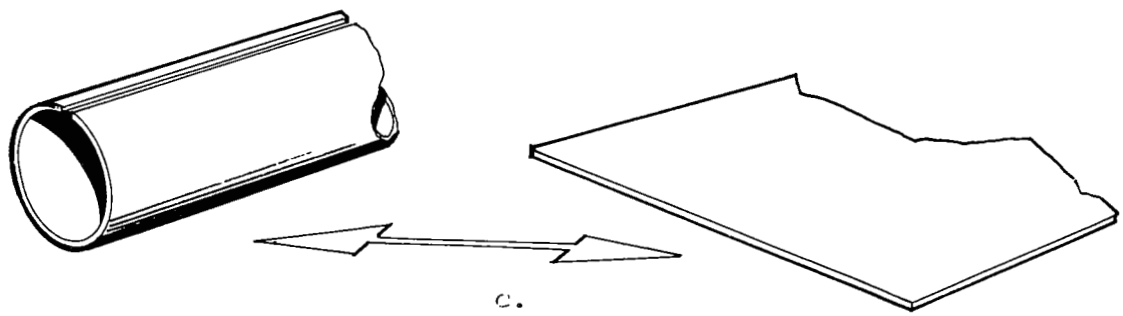

c.

Figure 16. Nitinol Concepts for Deploying Tubes

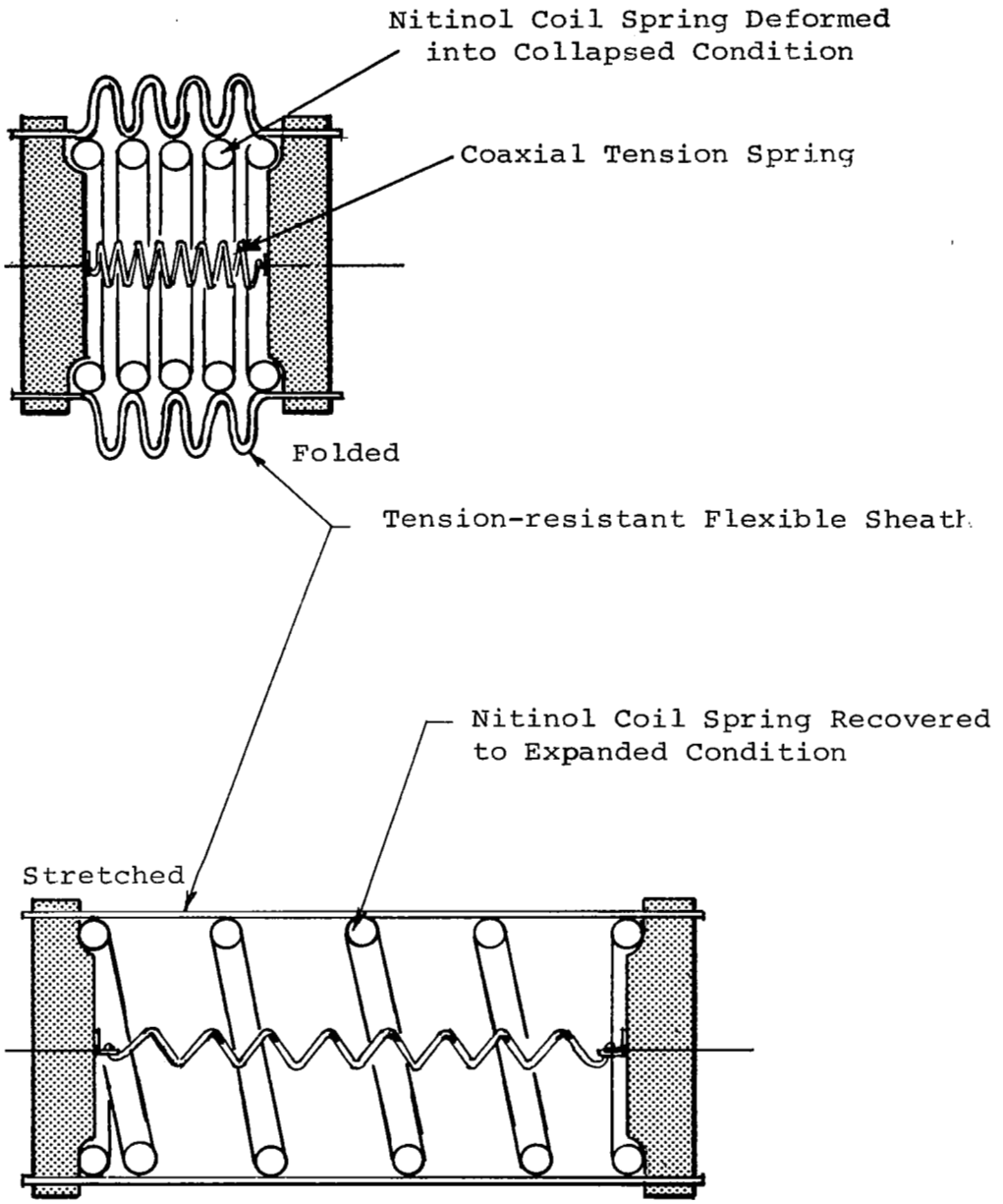

Figure 17. Deployable Nitinol Strut

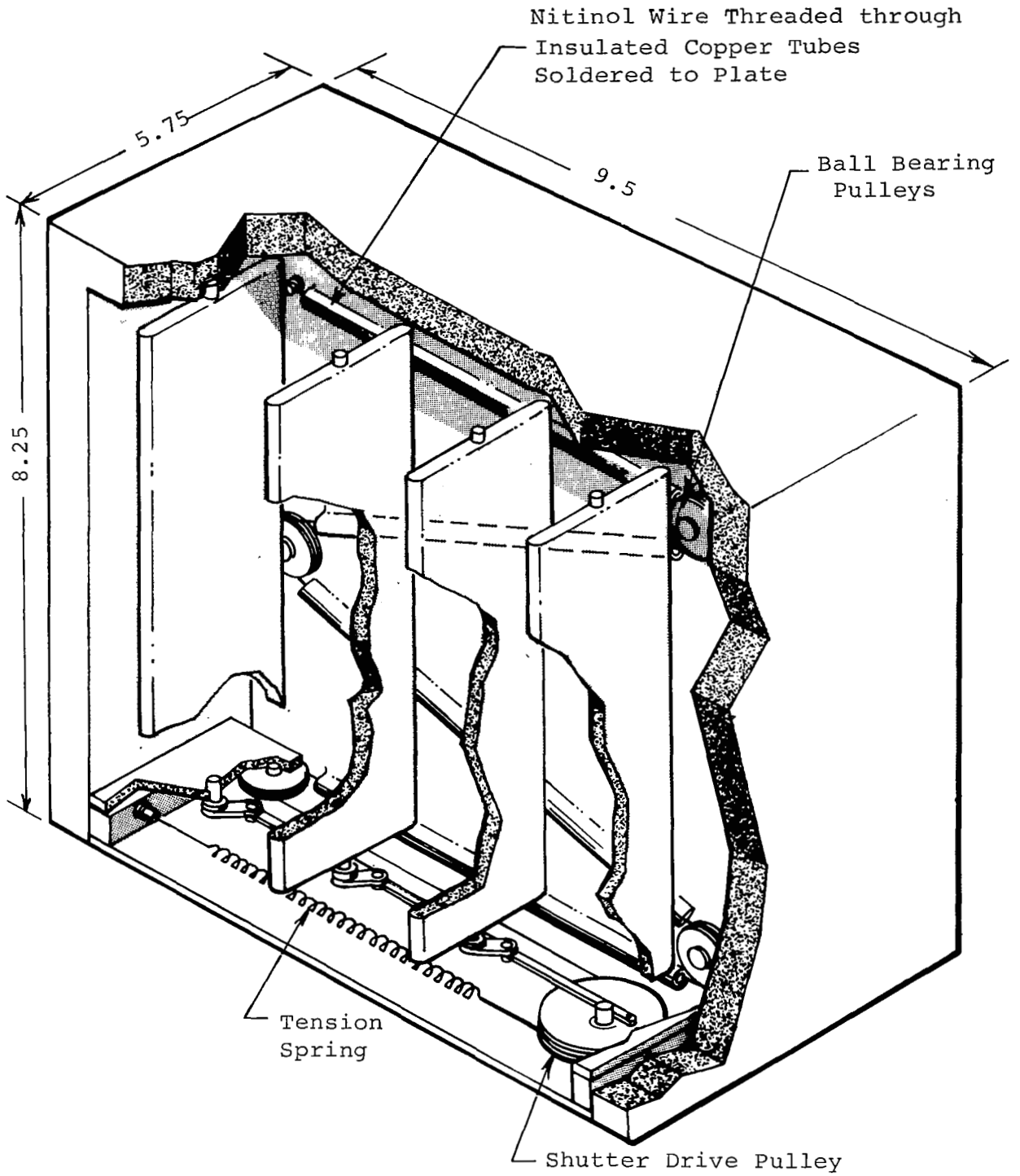

Figure 18. Semipassive Temperature Control Model Using Nitinol Wire

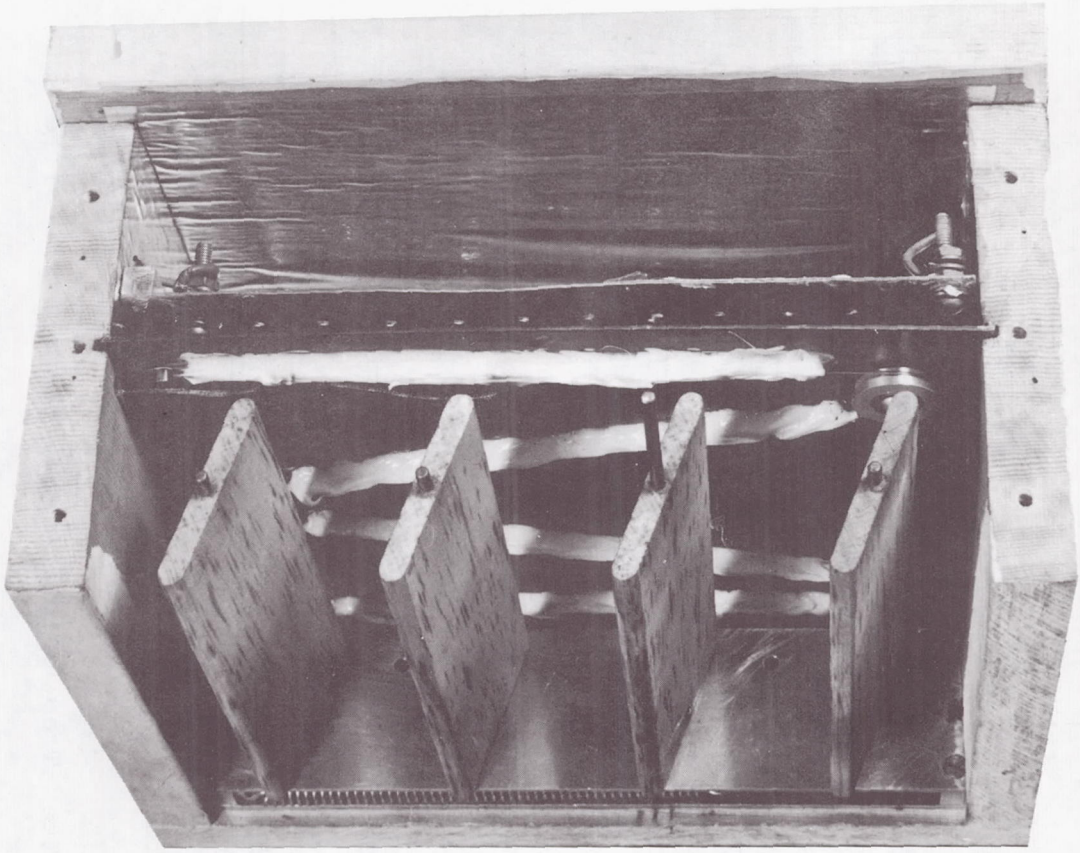

Figure 19. Model With Top Cover Removed Showing Copper Plate and Heating Element

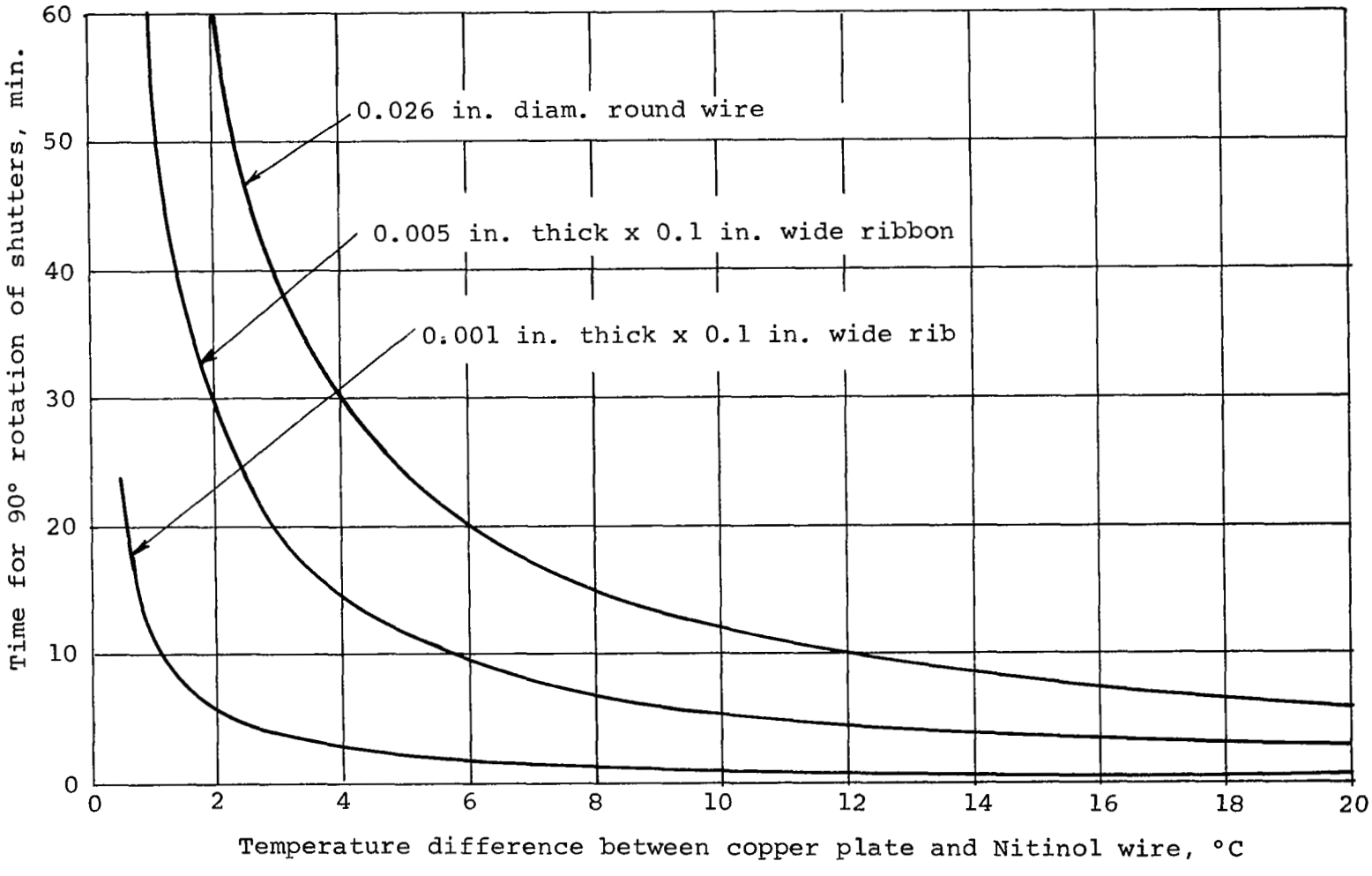

Figure 20. Shutter Travel Time versus Temperature Differential

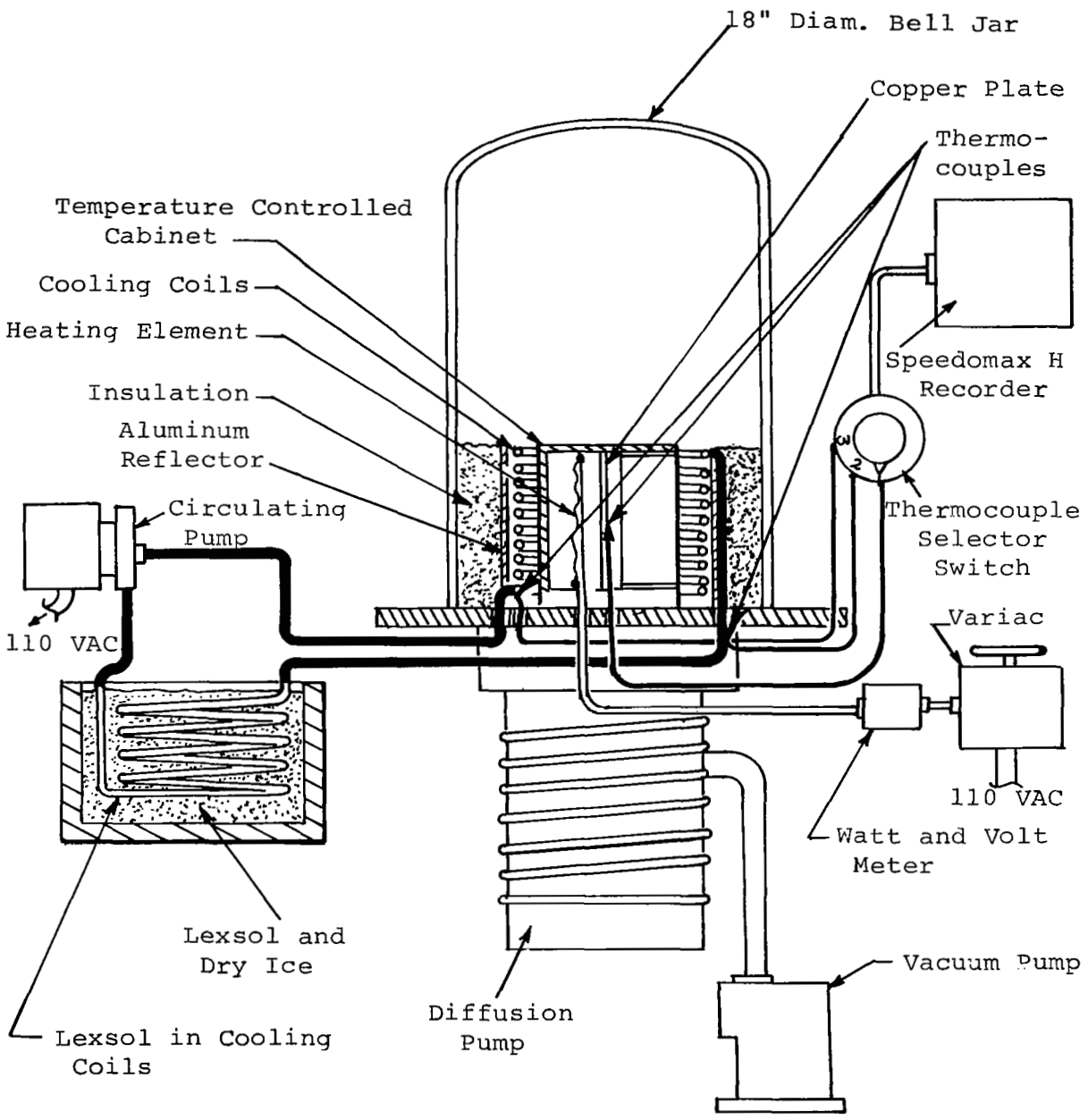

Figure 21. Test Apparatus for Temperature-Controlled Shutter Device

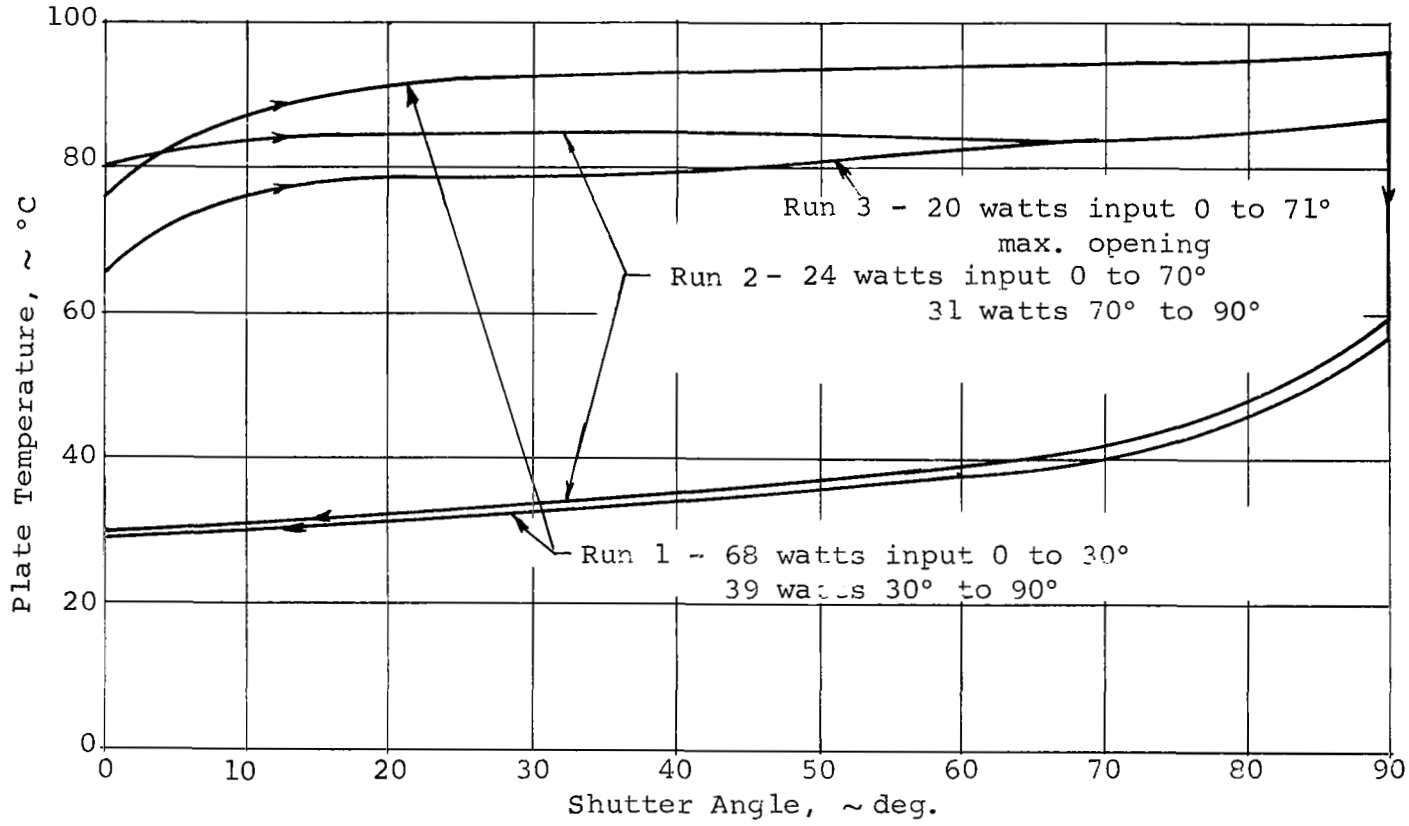

Figure 22. Variation of Shutter Angle with Plate Temperature

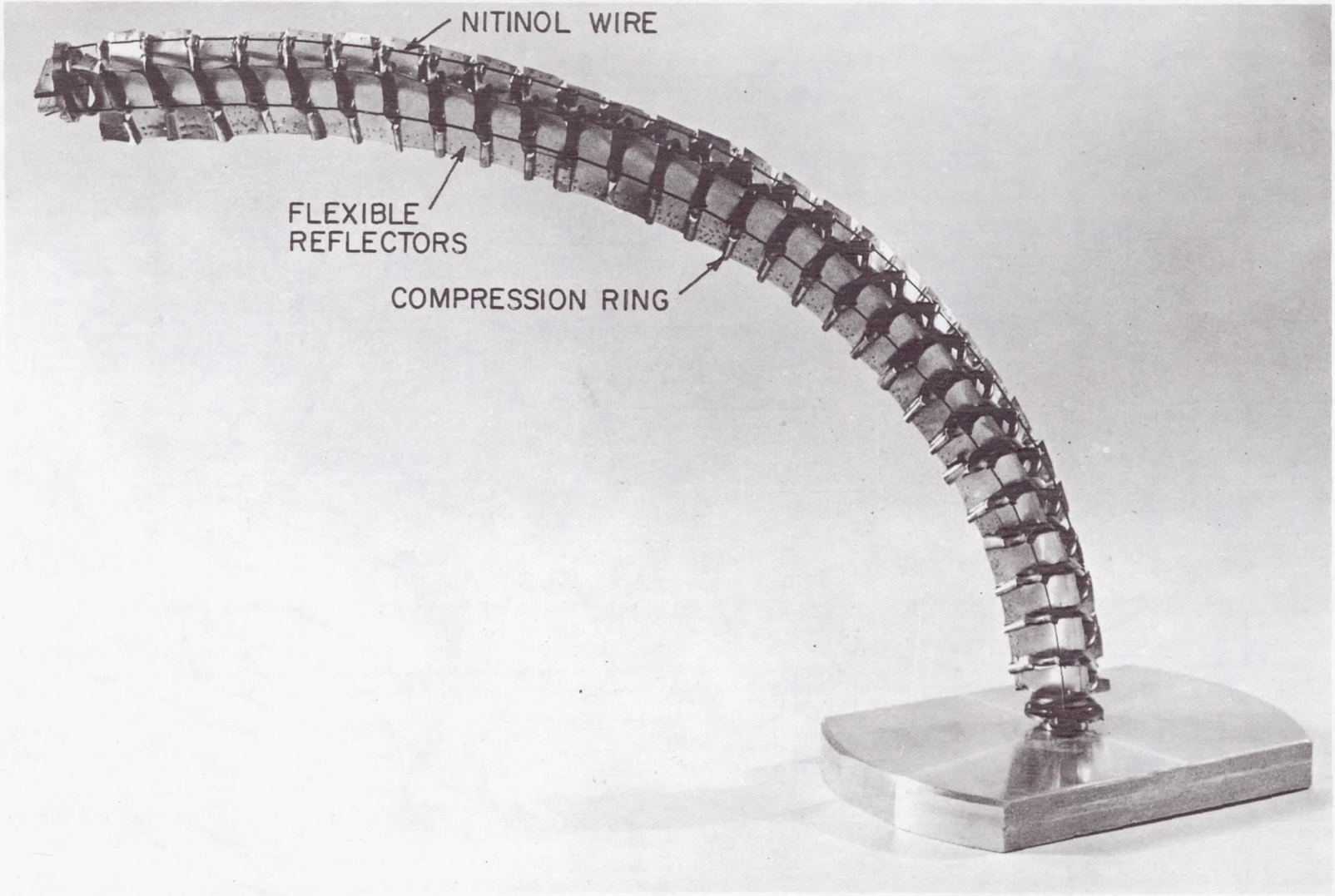

Figure 23. Photograph of Sun Seeker Device

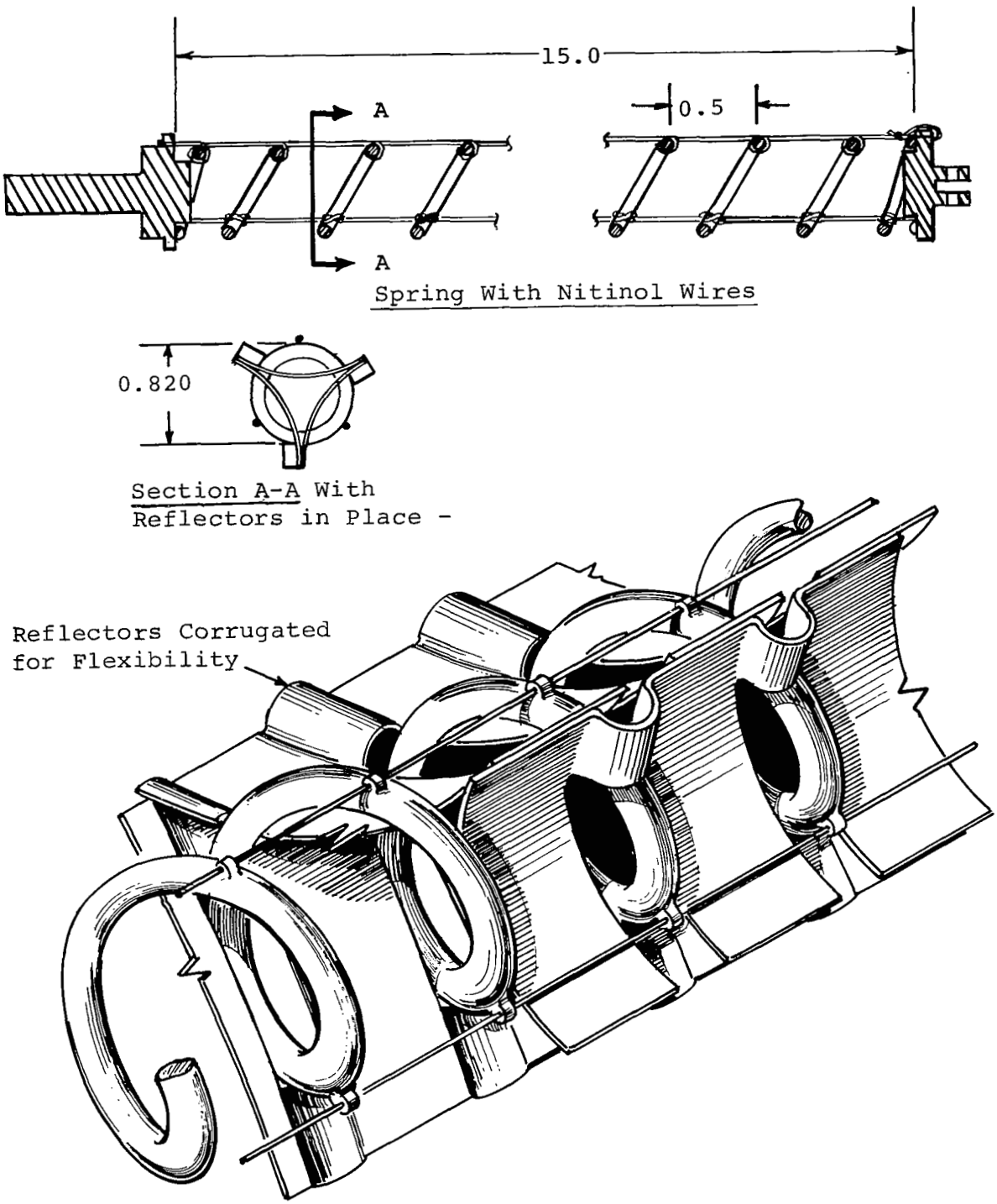

Figure 24. Sun Seeker Design Details

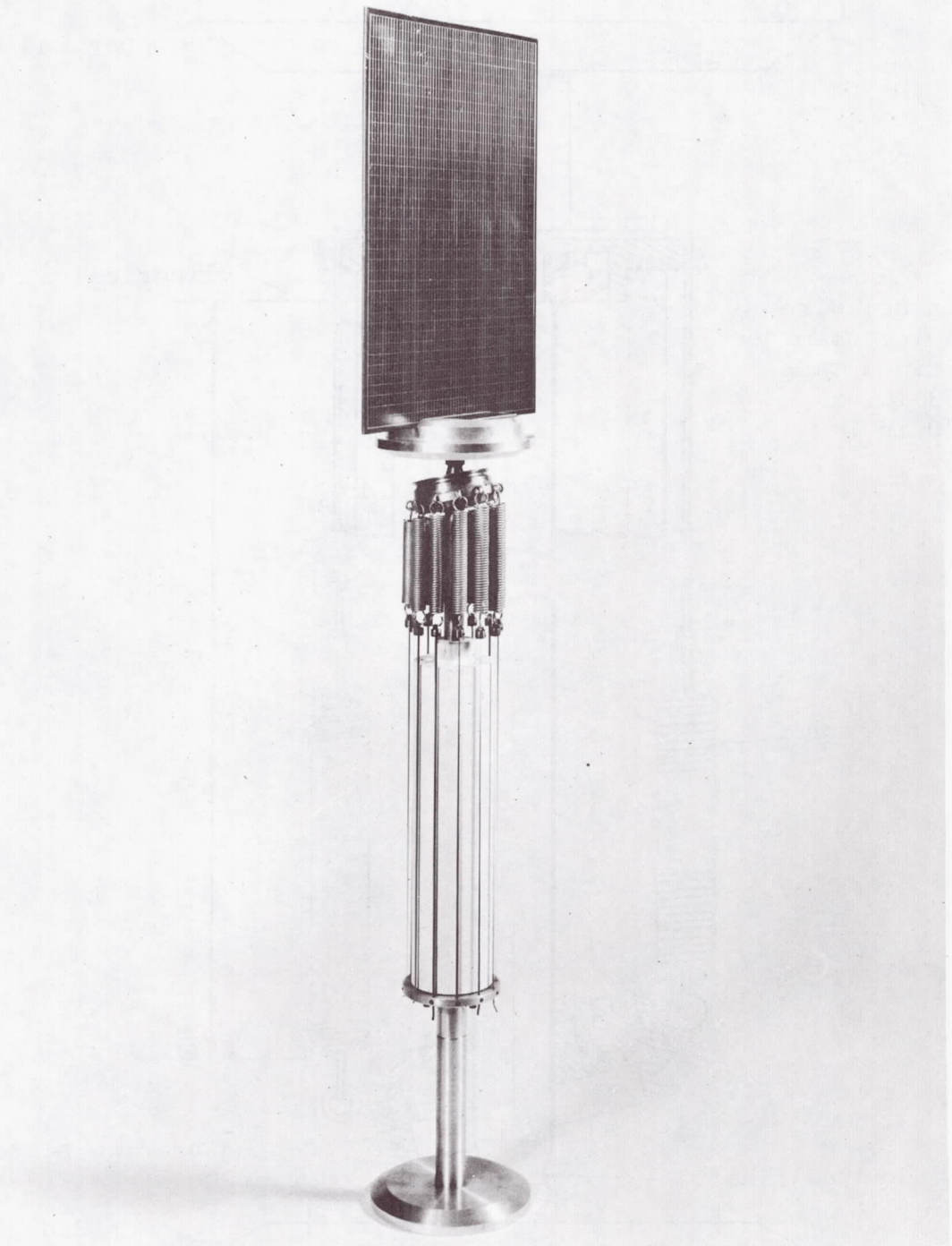

Figure 25. Photograph of Sun Follower Model

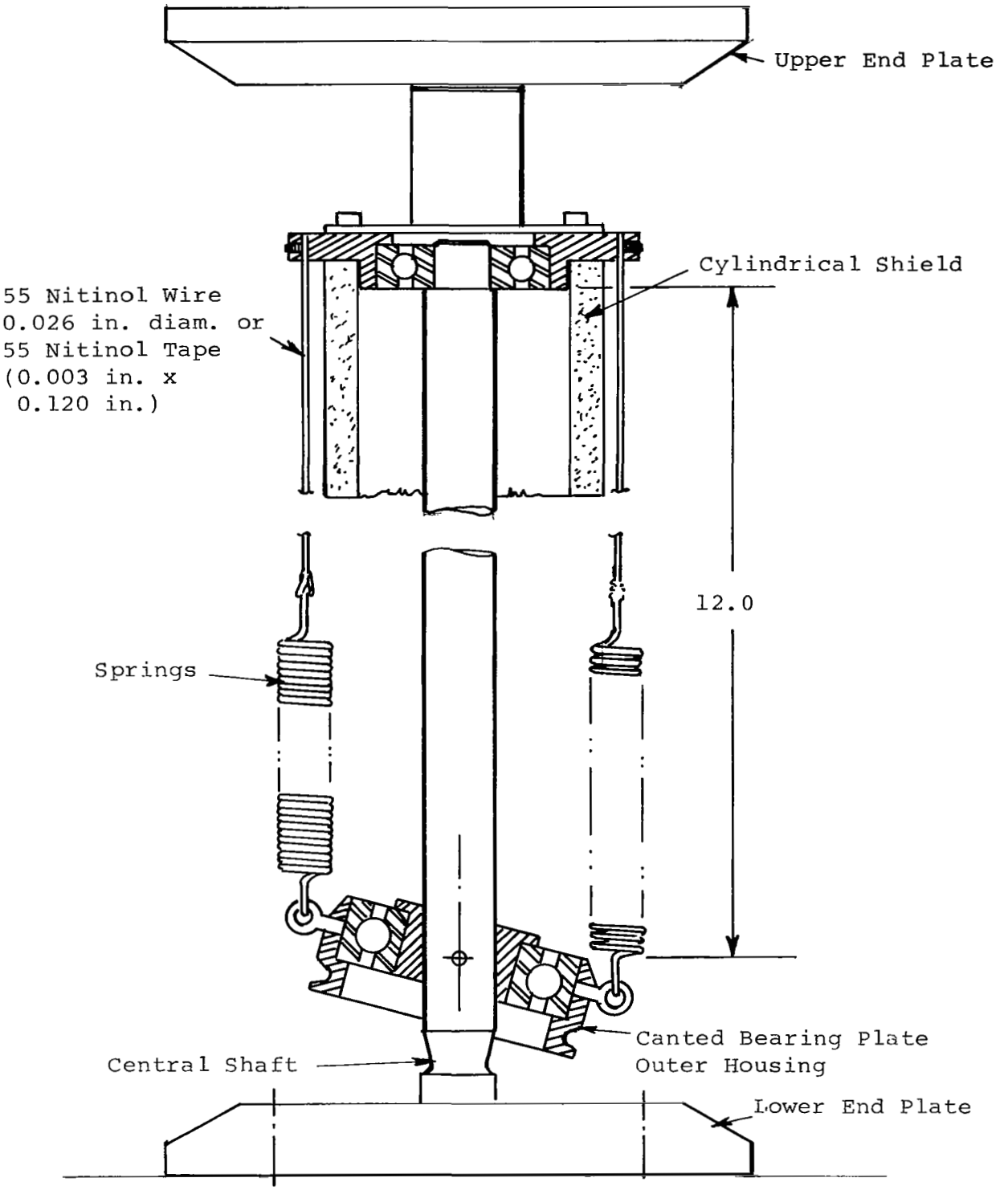

Figure 26. Engineering Layout Drawing of Sun Follower

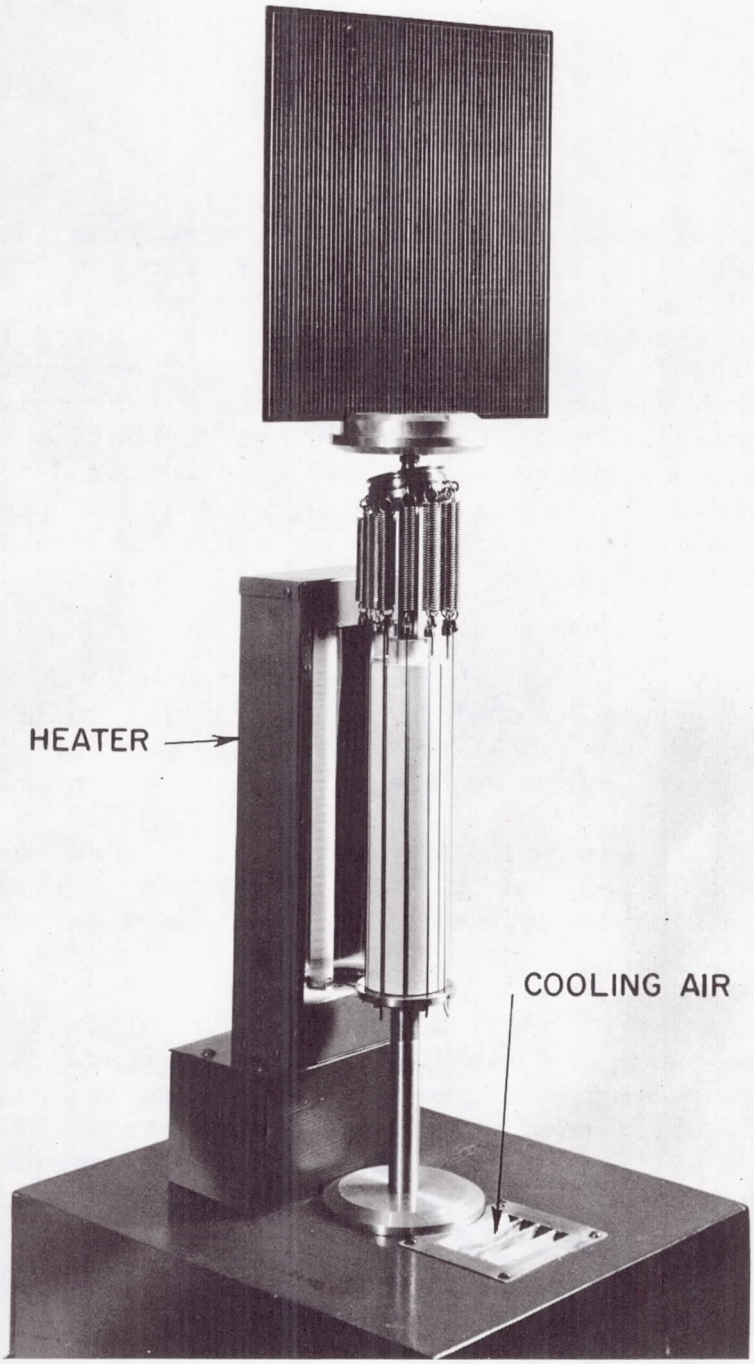

Figure 27. Photograph of Sun Follower Test Setup

APPENDIX A

TAPE FABRICATION

The Nitinol tapes were fabricated by rolling the wire in an experimental rolling mill designed and fabricated at Astro Research Corporation. The photograph of Figure A-1 shows the rolling mill with the feed side in the foreground. Wire was fed through a guide hole in the insulating block and between two copper rollers used to provide electrical contact. The set of pressure rollers formed a second electrode and provided the means for heating the wire. For hot rolling, the wire was maintained at a dull red heat prior to entrance. The wire was not heated after exit. Approximately 2-lb tension was applied to the wire to assist in drawing it evenly from the rolls. A uniform rolling speed of 1.6 ft/min was maintained.

Uniformity of ribbon thickness was found to be dependent upon the amount of reduction applied during initial rolling passes. Gradual reduction was obtained by multiple passes, each decreasing the cross-sectional area by about 5 percent of the original area.

Cold rolling was found to improve strain recovery properties. Samples were cold reduced by 10 to 15 percent in thickness by two additional cold passes after the last hot pass through the rolling mill.

Annealing was accomplished by heating in air in an electric furnace. The procedure was to adjust the furnace to the desired annealing temperature. The samples were then installed, and in approximately 0.5 minute the furnace had again reached the anneal temperature. After 4 minutes at the desired temperature, the specimens were removed. In order to prevent distortion and twisting, the ribbon was coiled to a diameter of about 3 in. and secured loosely with stainless-steel-wire ties at three points.

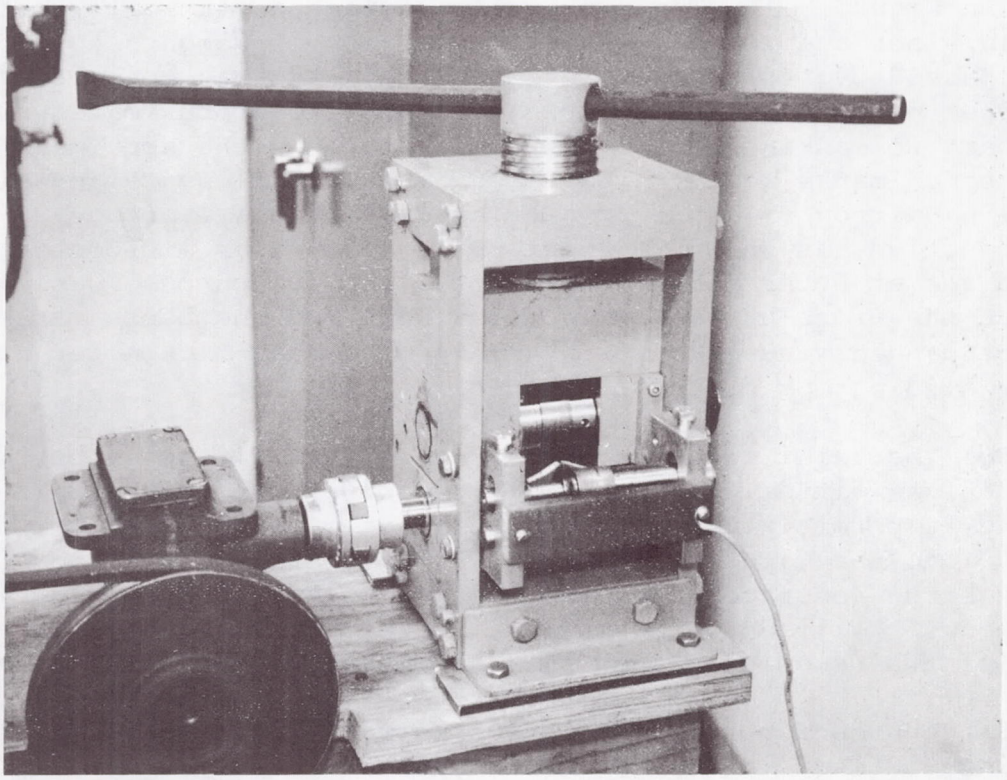

Figure A-1. Tape Rolling Mill

APPENDIX B

TEST EQUIPMENT AND PROCEDURES

The test equipment used for the axial stress-strain tests is shown in Figure B-1. The specimen was clamped vertically between two pin vises and loaded by the application of weights to a cord which passed over two low-friction pulleys and was connected to the upper pin vise. Bench marks were applied approximately 0.5 in. apart to masking-tape bands wrapped around the specimen. These bench marks were viewed through an optical system consisting of a Unitron filar micrometer eyepiece and a Gaertner 80 mm EFL objective, as shown in Figure B-2. The filar micrometer remained set at 0 throughout the tests since its purpose was only to provide the cross-hairs required for sighting the bench marks. Length changes were measured by means of a dial micrometer attached to the sliding optical system mount.

For the axial stress-strain tests of the Nitinol tape, the specimen was fitted with a crimp-type solderless ring terminal on one end to permit attachment of the loads. Gauge marks were indented into the tape approximately 3 in. apart. This gauge length was measured accurately and the specimen clamped vertically in the equipment. As loads were applied, the elongation was measured by means of two telemicroscopes with accompanying dial micrometers.

Procedures for the axial stress-strain tests consisted of applying the load in 2-pound increments and actuating an electric vibrator for 50 seconds prior to reading the resulting strain. The test temperature was monitored by a thermometer located near the specimen and remained relatively constant during all of the testing. After completing a loading cycle, the specimen would be heated in boiling water for 30 seconds without removing it from the fixture.

The torsional strain tests were conducted with the equipment shown in Figure B-3. To perform a test, the wire specimen was clamped vertically between two chucks which appear in the lower center of Figure B-3. Tape flags attached to the specimen provided a means for observing slippage in the chuck jaws. Weights were placed in either of the two cups (lower left) and the resulting load was transmitted through a cord to the torque drum (upper center). The drum was fixed to the torque shaft (center) which was mounted on two ball bearings and which was, in turn, attached to the upper chuck. The lower chuck was secured to a stationary

bracket connected to the apparatus frame by vertical tubes on either side of the torque shield. As each load increment was applied, an electric vibrator (left center) was actuated for a period of 60 seconds. This operation assists in the removal of friction effects at low load levels. Angular displacement was read from the upper surface of the torque drum which was scaled in 5° increments, from 0° to 360° in both positive (clockwise drum movement) and negative (counterclockwise drum movement) directions.

The procedure for the torsional stress-strain tests was to load in 2-gram increments to +30 grams and then unload in 2-gram increments. For half of the tests the specimen was then heated in boiling water for 10 seconds and allowed to cool to room temperature prior to reversing the loading in 2-gram increments to -30 grams. For the other half of the tests, the load was reversed without the intermediate heating cycle. After unloading from -30 grams in 2-gram increments, all specimens were heated for 10 seconds in boiling water. Each of the runs was repeated three times in rapid succession.

The equipment used in the temperature elongation tests is shown schematically in Figure A-5 and in the photograph of Figure A-6. The unit consists of two telescoping Pyrex tubes which enclose the specimen and which are free to slide vertically within two aluminum support brackets. The lower ends of the tubes are fitted loosely with brass plugs clamped to the specimen with set screws. Brass target washers are cemented to the upper ends of the tubes and provide the means for visually determining length changes which occur in that section of the specimen located between the set screws in the plugs. The assembly is supported by a tare load of 1.0 lb which is applied to the upper end of the specimen by means of a pin vise. A tensioning spring is provided to assure positive contact between the inner Pyrex tube and its plug by applying slight tension to the upper section of the specimen not used for measurement.

In operation, the apparatus is lowered into a Dewar flask containing a heat-exchanger coil and a liquid heat-exchange medium identified as Lexsol 408-M. The liquid level is maintained at the top surface of the upper support bracket. Axial strain is determined by measuring the relative displacement of two fine punch marks on the target washers or, alternatively, the displacement of the inner edges of the washers themselves. Measurement is accomplished with a Vickers AEI image-splitting eyepiece. The displacement measured is the change in length of that section of the specimen located between the brass plugs or, more specifically, between

the points at which the specimen first contacts the brass. This distance is determined by assembling the specimen in a jig which fixes the room-temperature length at 78.1 mm (3.075 in.). Axial strain measurements include length change for the outer Pyrex tube, but not for the inner tube in the region of the specimen. Accordingly, a thermal expansion value for Pyrex must be added to the measured data to obtain the actual strain value for the specimen under test.

The test temperatures were monitored with a Leeds and Northrup Speedomax H Millivolt recorder through two chromel-alumel thermocouples located near the ends of the specimen test section.

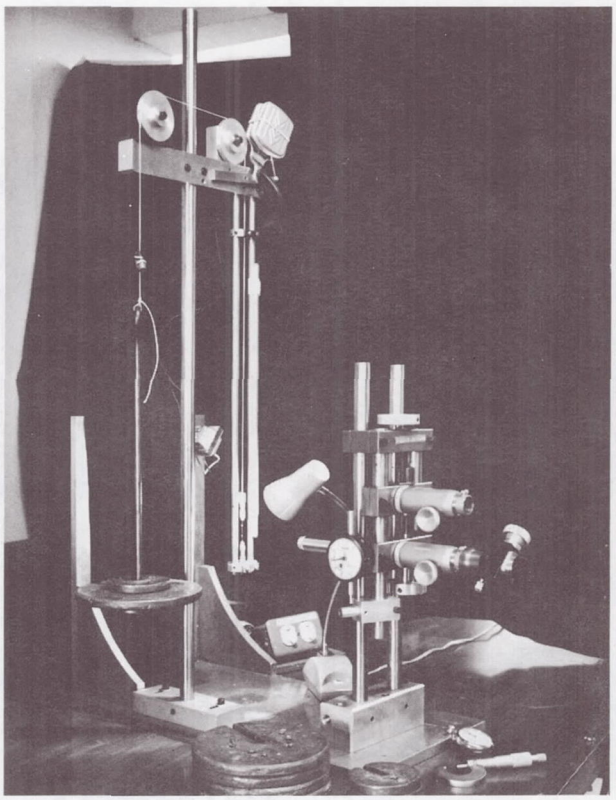

Figure B-1. Axial Stress-Strain Test Equipment

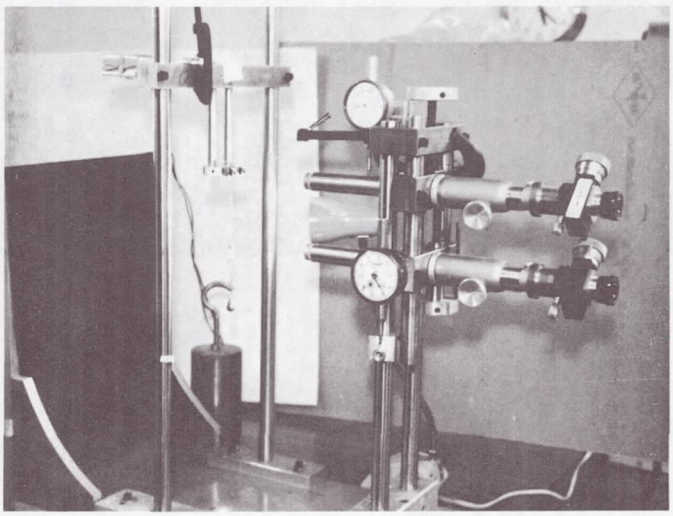

Figure B-2. Axial Strain Measuring Apparatus

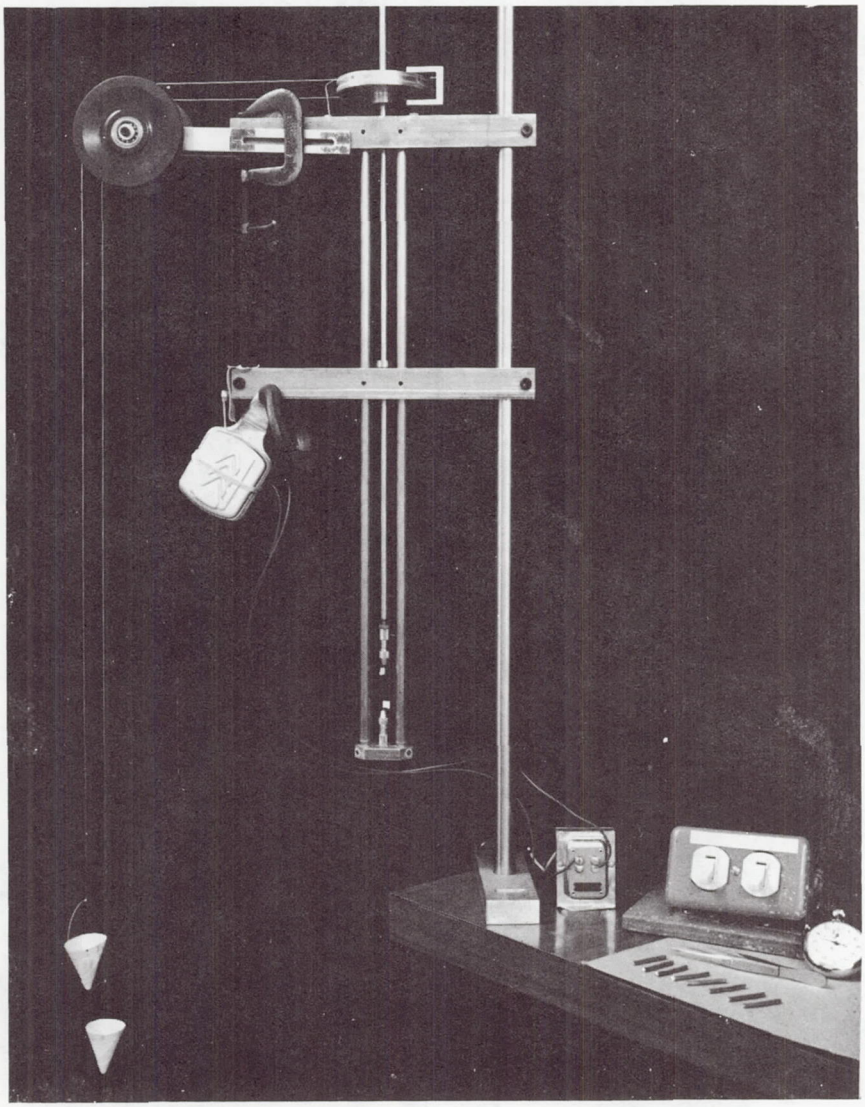

Figure B-3. Torsion Test Apparatus

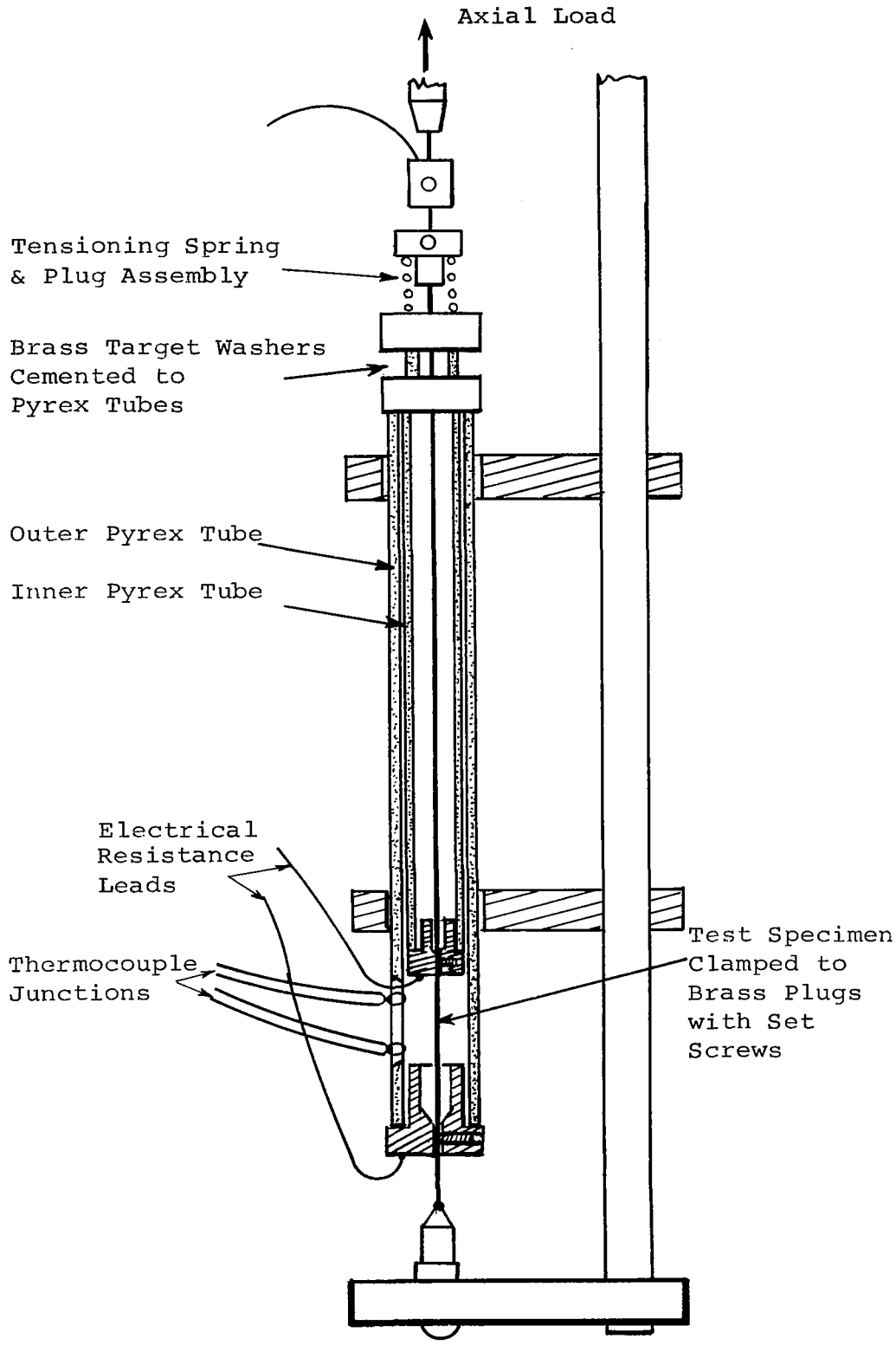

Figure B-4. Schematic Diagram of Temperature Elongation Equipment Removed from Temperature Control Bath

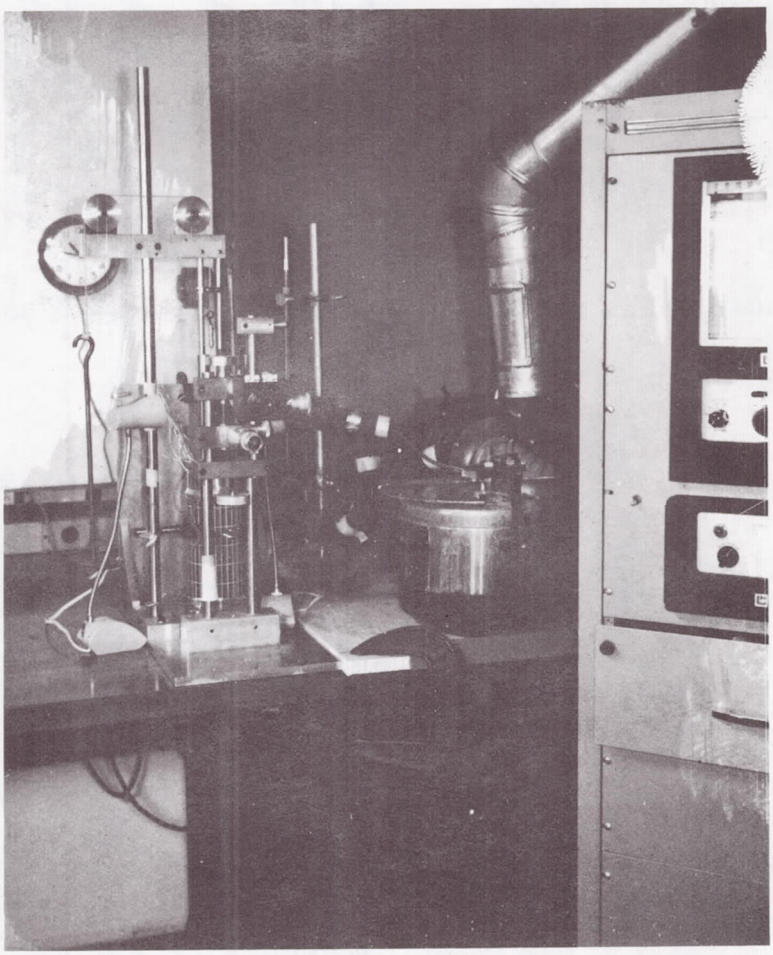

Figure B-5. Photograph of Temperature Elongation Test Equipment

REFERENCES

1. Buehler, W.J., Wiley, R.C., and Wang, F.E.: Nickel-Base Alloys, Patent No. 3,174,851, March 23, 1965.

2. NITINOL ALLOYS, Brochure from U.S. Naval Ordnance Laboratory, White Oak, Maryland, September 1965.

3. Buehler, W.J., and Wiley, R.C.: The Properties of TiNi and Associated Phases, Trans. ASM, Vol. 55, No. 2, June 1962.

4. Buehler, W.J., and Wang, F.E.: Martensitic Transformation in the TiNi Compound, Reactivity of Solids, Fifth International Symposium, Munich 1964.

5. Buehler, W., Private communication.

6. Wang, F.E.: The Mechanical Properties as a Function of Temperature and Free Electron Concentration in Stoichiometric TiNi, TiCo, and TiFe Alloys, Proc. First Interntl. Conf. on Fracture, Vol. 2, pp 899 - 908, 1965.

7. Wang, F.E., et al: Growth of TiNi Single Crystals by a Modified "Strain-Anneal" Technique, J. App. Phys. Vol. 35, No. 12, 3620, December 1964.

8. Buehler, W.J., and Wiley, R.C.: TiNi Ductile Intermetallic Compound, Trans. ASM, Vol. 55, No. 2, June 1962.

9. Buehler, W.J., et al: Effect of Low-Temperature Phase Changes on the Mechanical Properties of Alloys near Composition TiNi, J. App. Phys., Vol. 34, No. 5, 1475-1477, May 1963.

10. Goff, J.F.: Thermal Conductivity, Thermoelectric Power, and Electrical Resistivity of Stoichiometric TiNi in the 3° to 300°K Temperature Range, J. App. Phys, Vol. 35, No. 10, October 1964.

11. Mil. Spec. #MIL-N-81191 (WPP Nickel-Titanium Alloys, Low Magnetic Effects; Bars, Plates, Sheets, Strips, and Shapes (for Special Purpose Tools & Equipment), Rev. Dec. 1964.

12. Bradley, D.: Sound Propagation in Near-Stoichiometric TiNi Alloys, J. Acous. Soc. Amer., Vol. 37, No. 4, 700-702, April 1965.

13. Goldstein, D. M., et al: Effects of Alloying Upon Certain Properties of 55.1 Nitinol, U.S. Naval Ordnance Laboratory, White Oak, NOL TR 64-235, May 1965.

14. Rozner, A.G., et al: Effect of Addition of Oxygen, Nitrogen, & Hydrogen on Microstructure & Hardness of Cast TiNi Intermetallic Compound, Trans. ASM, Vol. 58, No. 3, September 1965.

15. Schuerch, H.U., and Hedgepeth, J.M.: Large Low-Frequency Orbiting Radio Telescope - Summary Report, Astro Research Corporation Report ARC-R-280, May 1968.

16. Sintes, J.F.: Flexural Instability of Foldable Tubes Based on the Elastic Recovery Concept, XVII Congress of International Astronautical Federation, October 1966.

17. London, A., and Drummond, F.O.,Jr.: Thermal System Design of the Nimbus Spacecraft, General Electric Missile and Space Division, presented at the XVII Congress of International Astronautical Federation, October 1966.

NASA-Langley, 1968 —— 17 CR-1232